AD_____

Award Number: DAMD17-98-1-8564

TITLE: Prostate-Specific Gene Therapy Using a "Gutless" Adeno-Vector Expressing Antisense TGF-Beta and PSA Promoter-Controlled TNF-Alpha Gene

PRINCIPAL INVESTIGATOR: Arie S. Belldegrun, M.D., FACS

CONTRACTING ORGANIZATION: University of California, Los Angeles
Los Angeles, CA 90095-1406

REPORT DATE: March 2002

TYPE OF REPORT: Annual Summary

PREPARED FOR: U.S. Army Medical Research and Materiel Command
Fort Detrick, Maryland 21702-5012

REPORT DOCUMENTATION PAGE

Form Approved
OMB No. 074-0188

1. AGENCY USE ONLY (Leave blank)	2. REPORT DATE	3. REPORT TYPE AND DATES COVERED
	March 2002	Annual Summary (1 Mar 01 - 28 Feb 02)

4. TITLE AND SUBTITLE
Prostate-Specific Gene Therapy Using a "Gutless" Adeno-Vector Expressing Antisense TGF-Beta and PSA Promoter-Controlled TNF-Alpha Gene

5. FUNDING NUMBERS
DAMD17-98-1-8564

6. AUTHOR(S)
Arie S. Belldegrun, M.D., FACS

7. PERFORMING ORGANIZATION NAME(S) AND ADDRESS(ES)
University of California, Los Angeles
Los Angeles, CA 90095-1406

E-Mail: abelldegrun@mednet.ucla.edu

8. PERFORMING ORGANIZATION REPORT NUMBER

9. SPONSORING / MONITORING AGENCY NAME(S) AND ADDRESS(ES)
U.S. Army Medical Research and Materiel Command
Fort Detrick, Maryland 21702-5012

10. SPONSORING / MONITORING AGENCY REPORT NUMBER

11. SUPPLEMENTARY NOTES
Report contains color.

12a. DISTRIBUTION / AVAILABILITY STATEMENT
Approved for Public Release; Distribution Unlimited

12b. DISTRIBUTION CODE

13. ABSTRACT *(Maximum 200 Words)*

The goal of this research has been to develop an immune-based gene therapy that combines targeted cytotoxicity with reversal of local tumor immune suppression to eradicate prostate cancer cells. Reversal of local tumor immune suppression was achieved *in vitro* by blocking the over expression of TGF-β2 produced by prostate cancer cells using TGF-β2 phosphorothioate oligonucleotide antisense. We have been developing a gutless adenovector with extended transgene expression that we think will have enhanced safety for pre-clinical and clinical use. Our gutless adenovector DNA backbone contains the cytotoxic gene under the control of an improved prostate specific promoter and a marker GFP gene for detection in *in vivo* studies. Our improved PSA promoter/enhancer presents 19-fold higher transcriptional activity compared to native PSA promoter/enhancer and has no loss of tissue specificity. Using Apo2L/TRAIL, a TNF-α related cytokine with less systemic toxicity, we have demonstrated selective cytotoxicity in our highly aggressive androgen-independent prostate cancer cell line (CL1). Further *in vivo* studies are being conducted to evaluate the overall efficacy and safety of Apo2L/TRAIL gene therapy in combination with TGF-β2 antisense for prostate cancer treatment.

14. SUBJECT TERMS	15. NUMBER OF PAGES
prostate cancer, gene therapy, adeno-vector, TGF-beta, TNF-alpha, viral gene delivery, TRAIL	34
	16. PRICE CODE

17. SECURITY CLASSIFICATION OF REPORT	18. SECURITY CLASSIFICATION OF THIS PAGE	19. SECURITY CLASSIFICATION OF ABSTRACT	20. LIMITATION OF ABSTRACT
Unclassified	Unclassified	Unclassified	Unlimited

NSN 7540-01-280-5500

Standard Form 298 (Rev. 2-89)
Prescribed by ANSI Std. Z39-18
298-102

Table of Contents

1. Zhang L, Adams J, Billick E, Ilagan R, Iyer M, Le K, Smallwood A, Gambhir S, Carey M, Wu L. Molecular Engineering of a Two-Step Transcription Amplification (TSTA) System for Transgene Delivery in Prostate Cancer. Molecular Therapy Vol 5, No 3, 223-232, 2002.
2. Pantuck A, Matherly J, Zisman A, Nguyen D, Berger F, Gambhir S, Black M, Belldegrun A, Wu L. Optimizing Prostate Cancer Suicide gene Therapy Using Herpes Simplex Virus Thymidein Kinase Active Site Variants. Human Gene Therapy. In press for May 2002.

Introduction:

Cancer gene therapy is the transfer to and expression of genetic material in malignant human cells for a therapeutic purpose. Hormone-refractory metastatic prostate cancer poses a tremendous therapeutic challenge. Clearly the development of novel therapies, such as gene therapy, is a high priority. Identifying and elaborating sophisticated selective gene therapy systems may amount to nothing unless genes can be targeted to a significant fraction of clonogenic cells. Viruses are attractive vehicles for gene delivery since they have evolved specific and efficient means of entering human cells and expressing their genes. Our laboratory has been developing approaches to delivery therapeutic genes to prostate cancer cells by harnessing the targeting efficiency of viruses, while abrogating their ability to cause infection and disease. Furthermore, we have been focusing on optimizing the PSA promoter, which was previously described in our laboratory, for tissue-specific expression in order to improve safety and specificity of prostate cancer gene therapy.

The transcriptional activity of tissue-specific promoters, including PSA promoter/enhancer, is much lower than constitutive viral promoters such as CMV. To improve the safety and efficacy of gene therapy *in vivo*, we developed a PSA promoter/enhancer with enhanced activity and good tissue-specificity. Based on principles of transcription regulation, we manipulated known PSA regulatory components by insertion and duplication of high affinity androgen-responsive elements (AREs) and by removal of intervening sequences between the enhancer and promoter sequences. Our *in vitro* studies demonstrate that our PSA-BC promoter/enhancer constructs not only exhibit 19-fold higher activity relative to the PSA promoter/enhancer control baseline, but also retained a high degree of tissue-specificity. [1]

Successful gene therapy approaches will require efficient gene delivery and sustained expression of the transgene in recipients. Lentiviruses belong to the family of retroviruses and capable of infecting nondividing cells.[2] With lentiviral vectors, sustained expression of transgene has been detected as long as 6 months.[3] Because lentiviral vectors can be pseudotyped with vesicular stomatitis virus G glycoprotein, they can transduce a broad range of tissues and cell types. Furthermore, this virus elicits minimal immune reaction. No inflammation or recruitment of lymphocytes could be detected at the site of injection. In addition, animals previously transduced with a lentiviral vector can be efficiently re-infected with lentiviral vectors.[3] Therefore, lentiviruses are ideal vectors for gene therapy because they offer efficient and sustained gene expression with minimal immunogenicity and toxicity.

TRAIL, also known as TNF-related apoptosis inducing ligand, is a cytokine belonging to the tumor necrosis factor (TNF) superfamily. TRAIL has the unique property of inducing cell-death in cancer cells yet spares normal cells.[4,5] Our group and others have reported that prostate cancer cells are susceptible to soluble recombinant TRAIL protein. [6-10] In fact, TRAIL has been shown to efficiently kill androgen-independent prostate cancer while TNF-α was essentially ineffective.[7] Therefore, TRAIL gene expression is a promising approach to target prostate cancer. Overall, by combining efficient viral gene delivery and tissue-specific expression, TRAIL gene therapy has the potential to become a safe and efficacious treatment for metastatic prostate cancer.

Body:

Task 1: Development of enhanced PSA promoters for tissue-specific expression by viral gene delivery.

The native PSA enhancer and promoter confer prostate-specific expression when inserted into adenovirus vectors capable of efficient in vivo gene delivery, although the transcriptional activity is low. By exploiting properties of the natural PSA control regions, we have improved the activity and specificity of the prostate-specific PSA enhancer for gene therapy and imaging applications. Our results have recently been published.[1] Our previous studies have established that androgen receptor (AR) molecules bind cooperatively to AREs in the PSA enhancer core (-4326 to -3935) and act synergistically with AR bound to the proximal promoter to regulate transcriptional output. To exploit the synergistic nature of AR action we generated chimeric enhancer constructs by (1) insertion of four tandem copies of the proximal AREI element; (2) duplication of enhancer core; or (3) removal of intervening sequences (-3744 to -2855) between the enhancer and promoter. By comparing to the baseline construct, PSE, containing the PSA enhancer (-5322 to -2855) fused to the proximal promoter (-541 to +12), the three most efficacious chimeric constructs, PSE-BA (insertion of ARE4), PSE-BC (duplication of core) and PSE-BAC (insertion of core and ARE4), are 7.3-, 18.9-, and 9.4-fold higher, respectively. These chimeric PSA enhancer constructs are highly androgen inducible and retain a high degree of tissue discriminatory capability. Initial biochemical studies reveal that the augmented activity of the chimeric constructs in vivo correlates with their ability to recruit AR and critical co-activators in vitro. The enhanced activity, inducibility and specificity of the chimeric constructs are retained in an adenoviral vector (Ad-PSE-BC-luc). Systemic administration of Ad-PSE-BC-luc into SCID mice harboring the LAPC-9 human prostate cancer xenografts shows that this prostate specific vector retained tissue discriminatory capability compared with a comparable cytomegalovirus (CMV) promoter driven vector.

Recently, we have made further advances in achieving maximal transcriptional activity and prostate specificity of tissue-specific promoter. Here we combine these technologies to create a robust, titratable, androgen-responsive system targeted to prostate cancer cells based on a two-step transcriptional activation (TSTA) system (Figure1). Our "chimeric" TSTA system uses a duplicated variant of the prostate-specific antigen (PSA) gene enhancer to express GAL4 derivatives fused to one, two, or four VP16 activation domains. We targeted the resulting activators to cells with reporter templates bearing one, two, or five GAL4 binding sites upstream of firefly luciferase. We monitored activity via firefly luciferase assays in transfected cell extracts and in live nude mice using a cooled charge-coupled device (CCD) imaging system. In this system, we found that firefly luciferase expression in prostate cancer cells can be varied over an 800-fold range (Figure 2). We also found that a single plasmid bearing the optimized

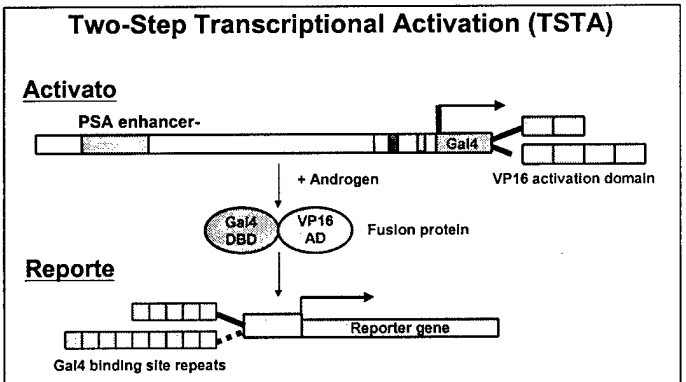

Figure 1: The TSTA system is composed of transcriptional activator component with artificial fusion protein driven by tissue-specific promoter and reporter (effector) component with multiple binding sites for fusion protein. The most important feature is its highly titratable nature in a wide range.

enhancer, GAL4--VP16 derivative, and reporter expressed firefly luciferase at 20-fold higher levels than the cytomegalovirus enhancer. We also generated the adenoviral vector expressing luciferase regulated by TSTA. Using a new optical CCD imaging, we documented that the in vivo transduction and expression mediate by TSTA is prostate specific and superior than CMV regulated expression (Figure 3). We are currently generating the TSTA regulated TKsr39 expression in adenovirus for use in microPET applications. Overall, the goal is to develop a potent prostate-specific promoter for the expression of heterologous genes for therapeutic applications and molecular imaging.

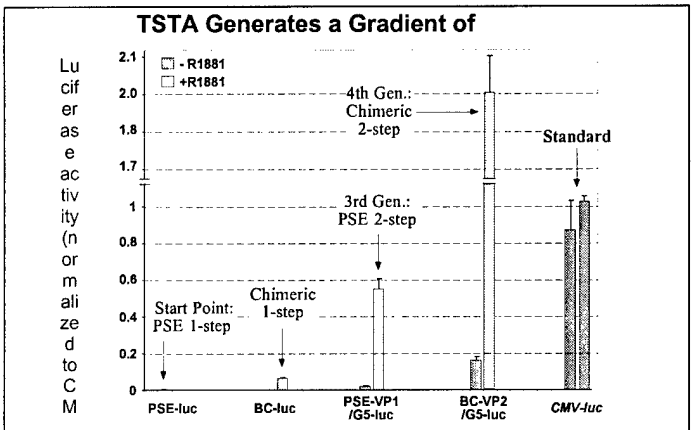

Figure 2: In our transfection study to human prostate cell line, the TSTA system showed over-800 hundred induction compared to the native one-step construct. Since they are driven by chimeric PSA promoter, they still retain tissue-specificity and androgen inducibility.

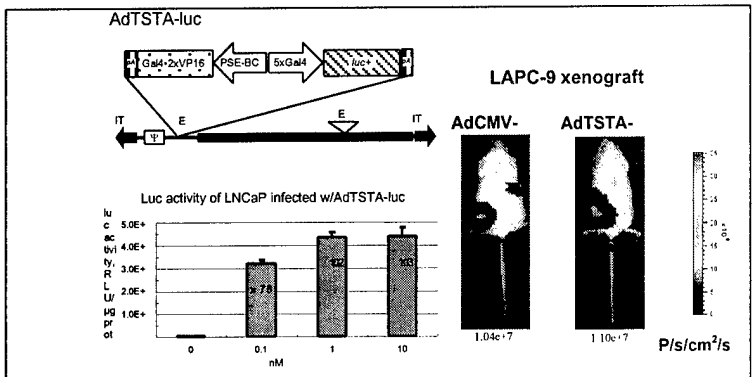

Figure 3: AdTSTA-luc is an adenovector carrying firefly luciferase driven by TSTA system. This virus showed an augmented activity, cell specificity, and androgen inducibility *in vitro* using LNCaP cells and comparable activity with AdCMV-luc *in vivo* with CCD-imaging system.

Task 2. *Evaluation of anti-tumor effects of TRAIL gene expression in vitro.*

We and others have shown that recombinant TRAIL protein caused cell death in prostate cancer cells. We investigated the potential use of gene expression of TRAIL as an anti-cancer agent capable of inducing apoptotic tumor cell death. As a proof-of-principle, we cloned the entire TRAIL gene behind the CMV promoter into an adenoviral expression system that also expressed the green fluorescent protein (GFP) as a way to follow which cells were infected. An adenovirus expressing only GFP served as the control. Figure 4 compares the cytotoxic effects of soluble recombinant TRAIL protein versus gene expression of TRAIL by adenovirus. The optimum amount of soluble TRAIL had been established previously.[8] While recombinant TRAIL at 100ug/mL caused 24% cell death, gene expression of TRAIL by adenovirus at a multiplicity of infection (moi) of 100 was responsible for nearly 80% cell death. TRAIL gene expression is superior to recombinant TRAIL in causing cell death. Figure 4B shows the change in morphology of cells expressing TRAIL by the Ad-TRAIL virus.

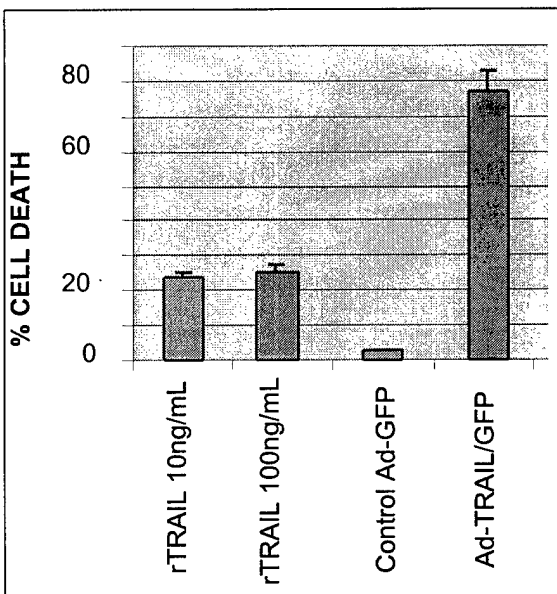

Figure 4A: PC-3 cells were incubated with recombinant Trail or adenovirus expressing GFP or TRAIL (100 moi) for 24 hours. Cell death was assayed by propidium iodide uptake using flow cytometry. Experiment done in triplicates

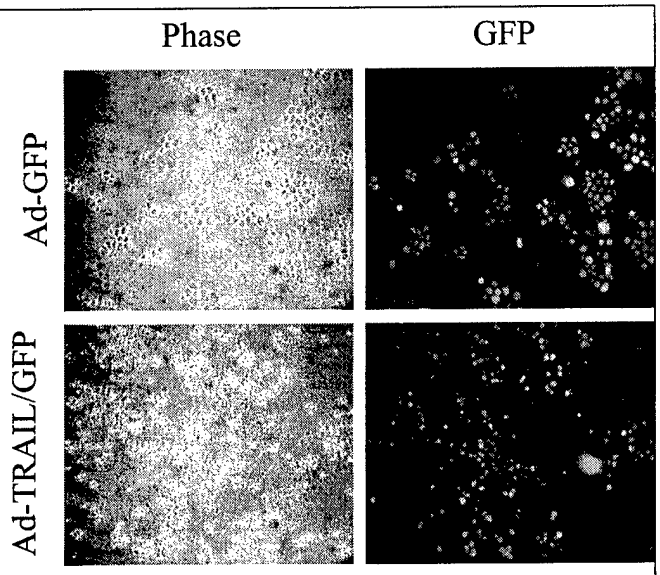

Figure 4B: Photographs of cells infected with control adenovirus and adenovirus expressing TRAIL after 24 hours of infection using 100 moi.

We wanted to determine why gene expression of TRAIL was more efficient than recombinant TRAIL at inducing cell death. Perhaps this was due to post-translational modifications which occurred as a result of gene expression which was not present in the recombinant TRAIL protein. In figure 5, PC-3 cells were infected with either control adenovirus or adenovirus encoding the TRAIL. After 24 hours of infection, the cells were harvested and fractionated by centrifugation into a supernatant and a membrane fraction. These subcellular fractions were applied to fresh uninfected PC-3 to determine if the cytotoxic effects were transferable. After 24 hours, the PC-3 cells were assayed for cell-death by flow cytometry. The membrane fraction of the adenovirus expressing TRAIL was able to confer nearly 80% cell-death while neither the supernatant nor the control virus caused significant cell death. To demonstrate that TRAIL expression was responsible for cell death, immunoprecipitation of the TRAIL-associated membrane fraction using polyclonal antibodies directed against TRAIL was able to effectively abrogate cell death (data not shown). In figure 6, the membrane fraction was analyzed by Western blot. Soluble TRAIL existed entirely as a monomer while gene expression of TRAIL produced oligomers with the majority being dimers. Therefore, gene expression of TRAIL produces a potent multimeric form of TRAIL that is membrane-associated. The membrane-associated quality of TRAIL is responsible for significant bystander cell death.

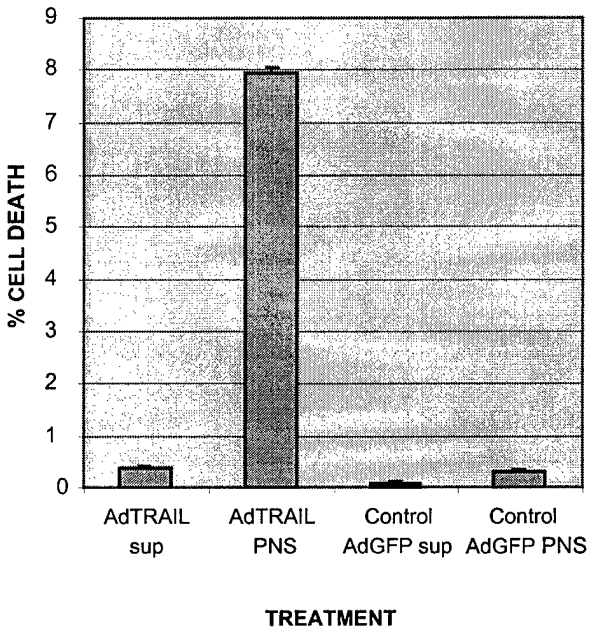

Figure 5: Bystander effect of TRAIL gene expression. PC-3 cells were infected with either Ad-GFP or Ad-TRAIL for 24 hours at 100 moi. The supernatant or membrane fraction from the infected cells were transferred to fresh uninfected PC-3 cells and incubated for 24 hours. Cell death was assayed by propidium iodide uptake using flow cytometry.

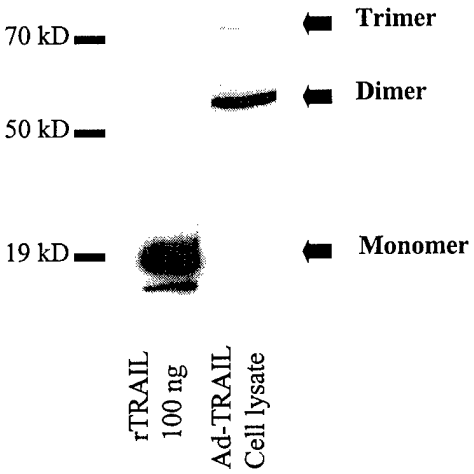

Figure 6: Western blot illustrating that soluble recombinant TRAIL exists as monomer. In contrast, TRAIL expression forms oligomers.

Task 3. *Development of viral vectors for gene expression under the control of PSA promoter/enhancer in order to improve safety and specificity of prostate cancer gene therapy.*

In our initial proposal, we described the development of a gutless adenoviral vector for the purposes of decreased vector immunogenicity. However, we have encountered major problems with viral genome recombination in generating our gutless adenovector prohibiting its practical use for gene delivery. An alternative approach utilizing lentiviral vectors was chosen which has proven to be more successful. Lentiviruses belong to the family of retroviruses which are capable of infecting nondividing cells, are capable of efficient gene expression and are of low immunogenicity. These qualities make lentiviruses ideal vectors for gene delivery. In collaboration with Dr. Inder Varma at the Salk Institute who kindly provided us with the vectors, we have successfully cloned the TRAIL gene into the lentiviral vector. Production of the VSV-G pseudotyped lentivirus encoding TRAIL involves transfecting 293T cells with three separate plasmids one encoding the therapeutic gene under the CMV promoter (pHR-CMV), one encoding the viral coat protein (pHR-VSV-G) and one encoding the structural proteins (p R) (Figure 7). Using this three-plasmid transfection approach, all lentiviruses generated are replication incompetent. Since all three plasmids are required to generate an infection-competent virus, this adds a considerable margin of safety for future clinical use.

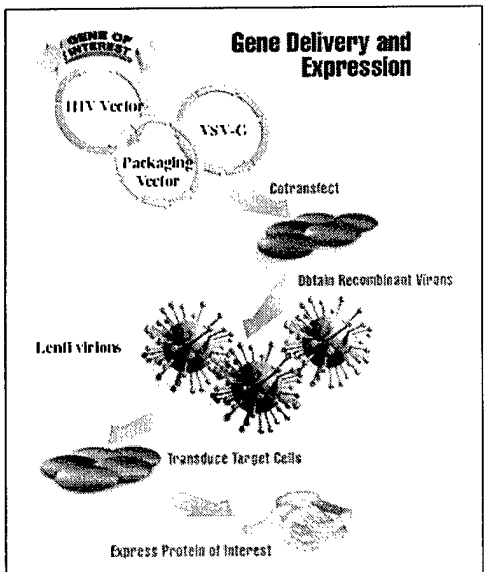

Figure 7: Production of pseudotyped Lentivirus involves cotransfection of 3 separate plasmids encoding the gene of interest, the VSV envelope protein and the packaging proteins.

Preliminary experiments with the lentivirus encoding TRAIL have shown that it is as efficient as adenovirus at inducing cell death. In figure 8, lentivirus expressing TRAIL was used to infect PC-3 cells at 100 moi. Cells were assayed at 48 hours post-infection to allow sufficient time for the lentiviruses to integrate into the host genome. Cell death was determined by the percentage of cells which incorporated propidium iodide. Lentivirus expressing TRAIL was responsible for 80% cell death compared to the control lentivirus expressing GFP which caused minimal cell death (2%). We are currently further characterizing the lentiviral system using similar approaches as described above TASK 2. In addition, we are planning to incorporate the optimized PSA promoter/enhancer into our lentiviral expression system.

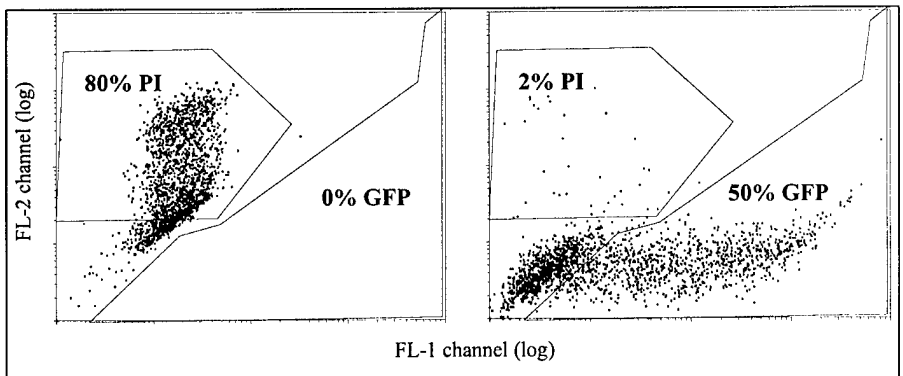

Figure 8: Flow cytometry assay for cell-death by uptake of propidium iodide uptake. Lenti-TRAIL virus (left panel) and Lenti-GFP virus (right panel) titers were normalized by ELISA assay for viral p24. PC-3 cells were infected at 100 moi and assayed for cell death at 48 hours.

Furthermore, in vivo animals using SCID mice are in progress. We will determine the efficacy of intratumoral and intravenous injection of both adenovirus and lentivirus encoding TRAIL at abrogating prostate cancer growth.

Key Research Accomplishments:

- Generation of chimeric PSA promoter/enhancer with improved transcriptional activity and tissue specificity.
- Creation of two-step transcriptional activation (TSTA) system which greatly increases PSA promoter/enhancer activity
- Demonstration in vitro that TRAIL gene expression is superior to TRAIL recombinant protein at inducing cell death. The potency of TRAIL molecule synthesized due to its oligomeric form which associates with cellular membranes to confer significant bystander cytotoxicity.
- Generation of a lentivirus expressing TRAIL which is capable of achieving significant cytotoxicity.

Reportable outcomes:

1. Manuscript: Wu L, Matherly J, Smallwood A, Adams JY, Billick E, Belldegrun A and Carey M: Chimeric PSA enhancers exhibit augmented activity in prostate cancer gene therapy vectors. Gene Ther. 8: 1416-26, 2001.
2. Manuscript: Zisman A, Ng CP, Pantuck AJ, Bonavida B and Belldegrun AS: Actinomycin D and gemcitabine synergistically sensitize androgen-independent prostate cancer cells to Apo2L/TRAIL-mediated apoptosis. J Immunother. 24: 459-71, 2001.
3. Manuscript: Zhang L, Adams JY, Billick E, Ilagan R, Iyer M, Le K, Smallwood A, Gambhir SS, Carey M and Wu L: Molecular Engineering of a Two-Step Transcription Amplification (TSTA) System for Transgene Delivery in Prostate Cancer. Mol Ther. 5: 223-32, 2002.
4. Manuscript: Bui, M, Sun, P, Ken, H, Nguyen, D, Zisman, A, Bonavida, B and Belldegrun, A: Lentiviral TRAIL gene expression for the treatment of androgen-independent prostate cancer. in preparation.

Conclusions:

The ultimate goal of achieving a safe and effective prostate cancer gene therapy requires multidisciplinary and multimodality approaches. We hope to achieve this goal along two simultaneous routes by optimizing our PSA promoter for tissue specific expression and by optimizing viral gene delivery. Together, both objectives will act synergistically to potentiate the anticancer effects of TRAIL and other therapeutic genes for the treatment of prostate cancer. Animal models will better evaluate the antitumor effects, therapeutic efficacy and safety with direct implications to future clinical trials. Overall, we have made significant progress and are intensifying our efforts to harness the utility of the tools generated to make prostate gene therapy a viable option in the near future.

References

1. Wu L, Matherly J, Smallwood A, Adams JY, Billick E, Belldegrun A and Carey M: Chimeric PSA enhancers exhibit augmented activity in prostate cancer gene therapy vectors. Gene Ther. 8: 1416-26, 2001.
2. Naldini L, Blomer U, Gallay P, Ory D, Mulligan R, Gage FH, Verma IM and Trono D: In vivo gene delivery and stable transduction of nondividing cells by a lentiviral vector. Science. 272: 263-7., 1996.
3. Kafri T, Blomer U, Peterson DA, Gage FH and Verma IM: Sustained expression of genes delivered directly into liver and muscle by lentiviral vectors. Nat Genet. 17: 314-7., 1997.
4. Gura T: How TRAIL kills cancer cells, but not normal cells. Science. 277: 768-768, 1997.
5. Nagane M, Huang HJS and Cavenee WK: The potential of TRAIL for cancer chemotherapy. Apoptosis. 6: 191-197, 2001.
6. van Ophoven A, Ng CP, Patel B, Bonavida B and Belldegrun A: Tumor necrosis factor-related apoptosis-inducing ligand (TRAIL) for treatment of prostate cancer: first results and review of the literature. Prostate Cancer and Prostatic Diseases. 2: 227-233, 1999.
7. Yu R, Mandlekar S, Ruben S, Ni J and Kong AN: Tumor necrosis factor-related apoptosis-inducing ligand-mediated apoptosis in androgen-independent prostate cancer cells. Cancer Research. 60: 2384-9, 2000.
8. Zisman A, Ng CP, Pantuck AJ, Bonavida B and Belldegrun AS: Actinomycin D and gemcitabine synergistically sensitize androgen-independent prostate cancer cells to Apo2L/TRAIL-mediated apoptosis. J Immunother. 24: 459-71, 2001.
9. Nesterov A, Lu XJ, Johnson M, Miller GJ, Ivashchenko Y and Kraft AS: Elevated Akt activity protects the prostate cancer cell line LNCaP from TRAIL-induced apoptosis. Journal of Biological Chemistry. 276: 10767-10774, 2001.
10. Munshi A, Pappas G, Honda T, McDonnell TJ, Younes A, Li Y and Meyn RE: TRAIL (APO-2L) induces apoptosis in human prostate cancer cells that is inhibitable by Bcl-2. Oncogene. 20: 3757-3765, 2001.

doi:10.1006/mthe.2002.0551, available online at http://www.idealibrary.com on IDEAL

Molecular Engineering of a Two-Step Transcription Amplification (TSTA) System for Transgene Delivery in Prostate Cancer

Liqun Zhang,[1] Jason Yeates Adams,[2] Erika Billick,[2] Romyla Ilagan,[1] Meera Iyer,[3] Kim Le,[1] Andrea Smallwood,[1] Sanjiv S. Gambhir,[3] Michael Carey,[1,*] and Lily Wu[2]

Departments of [1]Biological Chemistry, Box 1737, and [2]Urology, Box 1738, [3]Crump Institute for Molecular Imaging & Department of Molecular & Medical Pharmacology, Box 1770, University of California, Los Angeles School of Medicine, Los Angeles, California 90095-1737, USA

**To whom correspondence and reprint requests should be addressed. Fax: (310) 206-9598. E-mail: mcarey@mednet.ucla.edu.*

Gene therapy is founded on the concept that tissue-specific promoters can express heterologous genes for molecular imaging or therapeutic applications. The engineering of cell-specific enhancers to improve potency and the development of two-step transcriptional activation (TSTA) approaches have significantly improved the efficacy of transgene expression. Here we combine these technologies to create a robust, titratable, androgen-responsive system targeted to prostate cancer cells. Our "chimeric" TSTA system uses a duplicated variant of the prostate-specific antigen (PSA) gene enhancer to express GAL4 derivatives fused to one, two, or four VP16 activation domains. We targeted the resulting activators to cells with reporter templates bearing one, two, or five GAL4 binding sites upstream of firefly luciferase. We monitored activity via firefly luciferase assays in transfected cell extracts and in live nude mice using a cooled charge-coupled device (CCD) imaging system. In this system, we found that firefly luciferase expression in prostate cancer cells can be varied over an 800-fold range. We also found that a single plasmid bearing the optimized enhancer, GAL4–VP16 derivative, and reporter expressed firefly luciferase at 20-fold higher levels than the cytomegalovirus enhancer. We discuss the implications of this strategy and its application to molecular imaging and therapy.

Key Words: TSTA, GAL4–VP16, imaging, charge coupled device, gene therapy, prostate cancer

INTRODUCTION

The concept of tissue-specific gene therapy and imaging has been hampered by lack of specificity, borderline efficacy, and inadequate delivery methods. Improvements in all three areas must occur to translate the promise of gene therapy into meaningful clinical applications [1]. In prostate cancer, the most common strategy to control specificity of transgene expression is to use the regulatory region of a prostate gene product such as the prostate-specific antigen (PSA) [reviewed in 2]. To achieve optimal therapeutic efficacy, one goal of the field has been to achieve prostate-specific promoter activities similar in magnitude to those of ubiquitously active viral enhancers such as simian virus 40 (SV40) and cytomegalovirus (CMV) [3]. A logical and systematic approach to improve the PSA regulatory regions for combating prostate cancer involves several steps. Novel promoter constructs are engineered and their activity in cell-based transfection studies is evaluated. The most promising constructs are cloned into recombinant adenoviral vectors (or other efficient *in vivo* gene delivery vehicles) and tested in preclinical models [4,5].

We have recently initiated such studies for prostate cancer. We initially reported a strategy to augment the specificity and activity of the PSA enhancer by exploiting the synergistic nature of androgen receptor (AR) action. The key regulatory elements of the PSA enhancer include a proximal promoter (–541 to +12) comprising two binding sites for the androgen receptor (AREI and II) and a distal enhancer, which contains a 390-bp androgen-responsive core region [6,7]. The core region contains a cluster of closely spaced androgen response elements (AREs) and sites for other transcription factors [6–11]. The enhancer is active in both androgen-dependent (AD) and androgen-independent (AI) cancer cells [11]. AR binds cooperatively to the enhancer and mediates synergistic transcription [10]. Other factors within and outside of the enhancer contribute to prostate specificity [11,12–14]. We found that molecular engineering of the PSA enhancer by

1525-0016/02 $35.00

doi:10.1006/mthe.2002.0551, available online at http://www.idealibrary.com on IDEAL

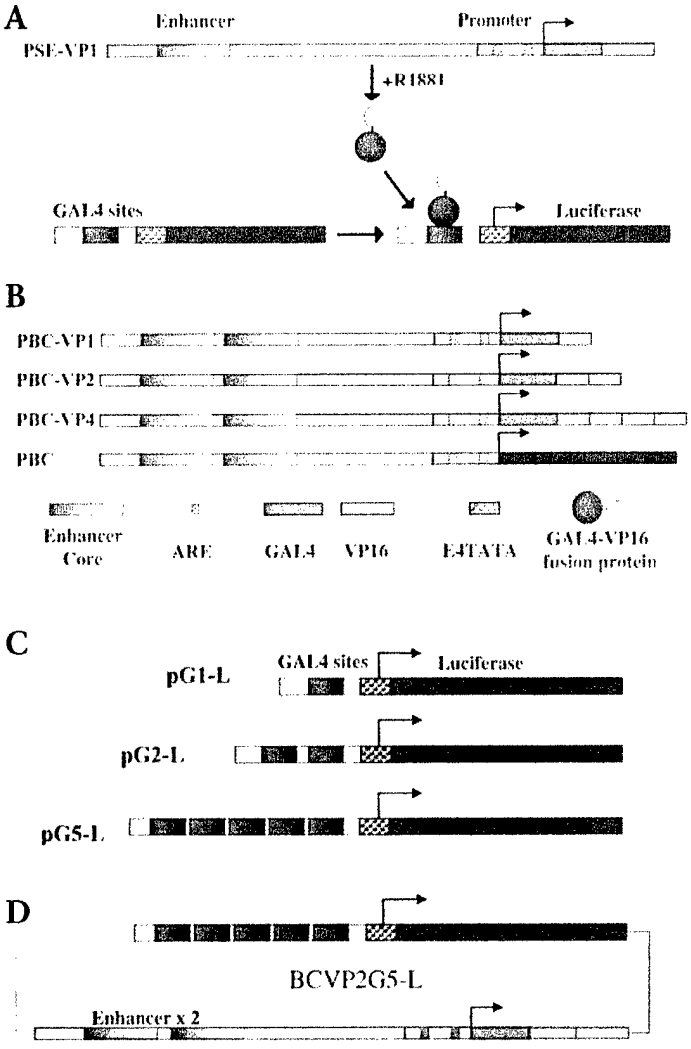

FIG. 1. Components of the chimeric TSTA system. (A) Depiction of the two-step transcriptional activation process. In the first step, GAL4–VP16 derivatives (oval circles) are expressed in prostate cancer cells in the presence of androgen (R1881), which activates the PSA enhancer, PSE. In the second step, GAL4–VP16 binds to a GAL4-responsive promoter and activates expression of luciferase. (B) The effector plasmids used in our analysis. GAL4, GAL4 DNA binding domain; VP16 AD, VP16 activation domain; Enhancer, the 390-bp core region bearing multiple AREs [10]; AREI and II, proximal AREs found in the promoter described in [6]. The GAL4-VP1 to -VP4 derivatives are as described [30]. E4TATA contains the adenovirus E4 minimal promoter from –38 to + 38 relative to the start site. (C) The FL reporters used in the analysis. (D) The single construct comprises the G5-L plasmid with the PBC-VP2 fragment inserted into the *Not*I site.

duplication of the core or fusion to multiple AREs generated 20-fold higher activities than the parental constructs yet retained androgen inducibility and tissue specificity [15]. Furthermore, we showed that the enhanced activity, inducibility and specificity of the chimeric constructs were maintained in an adenoviral vector expressing firefly luciferase (FL) [15].

The two-step transcriptional activation system (TSTA) is another strategy for augmenting PSA transgene expression (Fig. 1A) [16]. In the TSTA system, a potent transcriptional activator, which is driven by a cell-specific promoter, acts on a second expression plasmid, which encodes the reporter/therapeutic protein. This two-step approach results in cell-specific amplification of expression. The activator is often GAL4–VP16, a fusion protein comprising the DNA binding domain from the yeast transcription activator GAL4 and the activation domain from the herpes simplex virus 1 activator VP16. GAL4–VP16 assumes a unique specificity and potency that does not naturally exist in the mammalian cells [17,18]. The cell-specific TSTA approach is based on the original "enhancer trap" methodology used in *Drosophila melanogaster* to study developmental regulation of gene expression [19,20].

In one application of the TSTA approach to prostate cancer, the 5.3-kb intact PSA regulatory region was attached to GAL4–VP16 and androgen-dependent activation of a FL reporter gene bearing upstream GAL4 binding sites and ablation of cancer cells using a TSTA-driven toxic gene were demonstrated [21]. We used a similar TSTA expression approach but coupled it to imaging of prostate cancer in living mice. Prostate cancer cells injected into live mice were visualized using a cooled charge coupled device (CCD) optical imaging camera using a streamlined 2.4-kb PSA enhancer-promoter attached to a FL reporter [22]. In both cases, the TSTA system maintained androgen responsiveness, yet substantially amplified the signal versus the reporters driven directly by the PSA regulatory region.

Here, we sought to optimize the TSTA system for molecular imaging with eventual applications to therapy. Noninvasive molecular imaging with reporter genes can be used for imaging tumors and metastases, to monitor the therapeutic efficacy of drugs, cell trafficking, gene delivery and expression, as well as the study of various transgenic models [23]. Our objective was to augment the promoter activity and generate a titratable system. Augmented activity will be required to transition the FL-based CCD approach to clinically relevant methodologies such as positron emission tomography (PET). Titratability of expression, on the other hand, is an important safeguard in gene therapy. Often, the untoward side effects of introducing and expressing exogenous genes in animals and patients can not be fully predicted by *in vitro* or tissue culture experimentation. In addition, titratability is necessary because tumors and cell lines display varying AR responses [24,25]. For example, biphasic effects of androgen on AR activity have been observed and excess levels of androgen inhibit PSA production and cell growth [26]. A study on the LNCaP subline also suggests

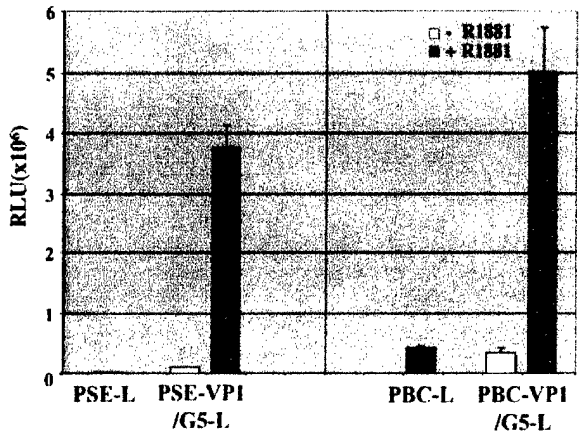

FIG. 2. Comparison of two-step versus one-step. We grew LNCaP cells in 6-well tissue culture plates and transiently transfected them with G5-L reporter and PSE/PBC-driven GAL4-VP1 (two-step), or with luciferase reporter driven directly by PSE/PBC (one-step). We added 10 nM R1881 (synthetic androgen) to the "+ ligand" samples 1 hour after transfection, and measured the luciferase activities 48 hours after stimulation. The experiments were repeated multiple times in triplicate. The measurements shown here are average values of a representative experiment. The vertical axis shows the relative light unit (RLU) reading from the luminometer. The error bars represent standard deviation.

that chronic androgen treatment induces reversible cell adaptation to the stimulant [27]. An additional complexity is that excess GAL4–VP16 exhibits a transcriptional inhibitory effect called squelching [28], which can generate cell toxicity and might confound TSTA under certain conditions [29].

The concept of adjusting transgene expression by controlling the activator and promoter potency is detailed in older studies on GAL4-derived activators [18]. In a subsequent study, a wide range of activities was generated by exploiting the synergistic behavior observed by varying the number of activation domains on the GAL4-derived activator and GAL4 binding sites on the reporter plasmid [30]. Here we combine the modified GAL4 system with natural and chimeric PSA enhancers to create a highly active, robust expression system for prostate cancer gene imaging and therapy. We demonstrate the cell specificity, efficacy, and utility of this system by imaging living mice using cooled CCD optical technology.

RESULTS

The Chimeric TSTA System

There are four primary variables in the TSTA system: 1) the potency of the prostate-specific promoter driving GAL4–VP16 (the effector; Fig. 1B); 2) the number of GAL4 binding sites proximal to the FL reporter gene (Fig. 1C); 3) the potency of the GAL4–VP16 derivative (Fig. 1B); and 4) the presence of the effector and reporter genes on the same plasmid (Fig. 1D). Each variable offers a unique opportunity to modulate gene expression.

We used two variants of the tissue-specific PSA promoter (Fig. 1B). The first is PSE, which contains a 2.4-kb fragment (–5824 to –2855), encompassing the 390-bp core PSA enhancer core region (–4326 to –3935), linked to the proximal PSA promoter (–541 to +12). The second, PSE-BC (abbreviated as PBC here) [15], contains the PSA enhancer with a duplicated 390-bp core but a deletion of an 890-bp intervening sequence between the enhancer and promoter (–3743 to –2855). These modifications augmented androgen-responsive expression 20-fold in cell culture [15].

The reporter templates contain the FL gene under the control of one, two, or five copies of the 17-bp GAL4 binding sites positioned 23 bp upstream of a minimal promoter containing the adenovirus E4 gene TATA box (Fig. 1C) [30]. The resulting plasmids are termed G1-L, G2-L, and G5-L. We used PSE and PBC to express recombinant GAL4–VP16 variants to generate a series of effector plasmids that display a gradient of activities (Fig. 1B). PSE expresses the 147-amino-acid GAL4 DNA binding domain (DBD) bearing a single copy of the 42-amino-acid VP16 activation subdomain (amino acids 413–454), PSE-VP1 [30]. We engineered PBC to express GAL4 DBD fusion proteins containing one, two, or four copies of the VP16 subdomain. We abbreviated the resultant plasmids as PSE-VP1, PBC-VP1, PBC-VP2, and PBC-VP4 and cloned the optimal combination of PBC-VP2 and G5-L into a single plasmid termed PBCVP2G5-L.

We expressed the parental plasmids GAL4-VP1, -VP2, and -VP4 from the SV40 enhancer as positive controls to provide a benchmark for comparison. As an additional benchmark, we used a FL construct driven by the CMV enhancer termed CMV-L. We systematically evaluated the TSTA constructs by co-transfection assays into the androgen-responsive prostate cancer cell line, LNCaP, in the presence of 10 nM R1881. We normalized each experiment using either CMV-L or SV40 constructs and graphed representative individual experiments. Subsequently, we tested several cell lines to evaluate cell specificity. For ease of comparison with the TSTA system, we will refer to PSE or PBC directly driving FL expression as the one-step system.

Evaluation of the Variables

We evaluated the variables to determine the relative efficacies of the one- versus the two-step systems; the use of PSE versus PBC to drive GAL4–VP16 expression; the effect of varying the number of GAL4 binding sites; and the effect of varying the number of VP16 activation domains.

The TSTA system displayed enhanced activity and androgen inducibility versus the one-step system in transfection assays. Cotransfection of PSE-VP1 and G5-L resulted in an activated level in cell culture that was 250-fold greater than the PSE-L one-step construct (Fig.

doi:10.1006/mthe.2002.0551, available online at http://www.idealibrary.com on IDEAL

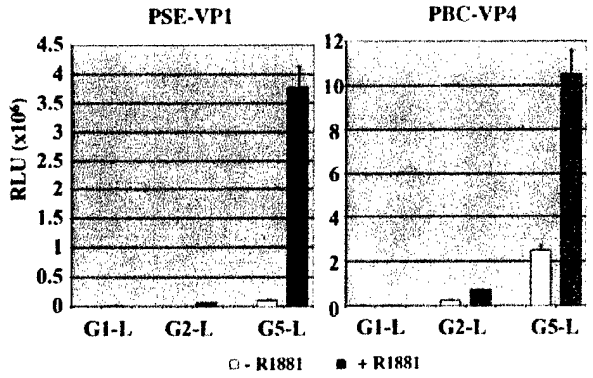

FIG. 3. Increasing the number of GAL4 sites and VP16 domains augments activity. We transfected LNCaP cells with PSE-VP1 (left) or PBC-VP4 (right) and G1-, G2-, and G5-L. We treated and measured the cells as in Fig. 2. The measurements shown in the two panels are from a side-by-side experiment.

2). Further, the TSTA system retained strong androgen-responsiveness (compare + and –R1881). However, the PBC-VP1/G5-L combination exhibited an induced activity only 15-fold better than the PBC-L. Comparison of PSE-VP1 and PBC-VP1 on G5-L revealed only a 1.5-fold difference, which is not considered significant ($P = 0.1$). This value was much less than the 20-fold difference observed between PSE-L and PBC-L [15], suggesting that despite the augmented potency of PBC, the FL levels in LNCaP cells begin to saturate with G5-L as a reporter.

Variation of the number of GAL4 binding sites contributed to the titratability (Fig. 3). The activity with PSE-VP1 increased nearly eightfold after increasing the number of sites from one (G1-L) to two (G2-L). However, raising the number of sites from two (G2-L) to five (G5-L) increased the activity an additional 60-fold. The pattern changed when examining the combination of a stronger promoter, PBC, and a more potent activator, GAL4–VP4. In this example, the largest increase in activity, 30-fold, was observed from G1-L to G2-L. From G2-L to G5-L there was only a 15-fold increase. The activity seems to saturate at five GAL4 sites because G9-L exhibited the same activity as G5-L with PBC-VP2 as an effector (data not shown). PSE-VP1 and PBC-VP4 both increase transcription activation synergistically as the number of activator binding sites increases. The magnitude of the synergy and the absolute level of activation, however, are related to the potency of the effector plasmid, providing a strategy to further adjust the expression levels in this system.

The final parameter we measured was the effect of multimerizing the VP16 activation domain (Fig. 4). With G5-L as reporter, PBC-VP2 displayed a threefold greater activity than PBC-VP1 ($P = 0.0007$). PBC-VP2 is modestly better than PBC-VP4 ($P = 0.02$), possibly because PBC-VP4 is causing an inhibitory phenomenon called "squelching" [28]. Nevertheless, the hallmark was the combination of PBC-VP2 and G5-L, where the level of activated expression reproducibly exceeded the activity of both benchmarks (CMV-L and the combination of SV40-VP4 with G5-L). Figure 5 illustrates the full spectrum of expression levels observed in our system, with an 800-fold variation from the weakest one-step to the strongest two-step system.

Tissue and Cell Specificity of the TSTA System

We chose the TSTA combination of PBC-VP2 and G5-L for analysis of tissue specificity (Fig. 6). We compared prostate and non-prostate lines, and cell lines expressing and lacking AR to assess authentic prostate specificity and distinguish it from simple androgen responsiveness. The LAPC4 cell line is an advanced prostate cancer cell (tumor cells from patient with refractory/metastatic prostate cancer) line that expresses AR and displays modest androgen-responsiveness as measured by PSA induction [31]. The mammary carcinoma cell line MCF-7 also expresses AR but not PSA. The human cervical cancer cell line, HeLa, is negative for AR and PSA. fAR-HeLa expresses flag-tagged human AR but not PSA [10]. Finally, we included the human hepatic cell line HepG to test for potential activity in liver.

During our initial tests we discovered that CMV-L responds to androgen stimulation (Fig. 4 and data not shown). We used SV40-driven GAL4–VP2 and G5-L as a benchmark to properly normalize experiments in different cell types. The SV40-VP2/G5-L displayed a similar activity as CMV-L in LNCaP and was not significantly affected by androgen in any cell lines tested. In LNCaP cells, we consistently observed that, in the presence of androgen, the combination of PBC-VP2 and G5-L had an activity that was similar to that of SV40-VP2 and G5-L (Fig. 6B). This observation was consistent with immunoblot analysis

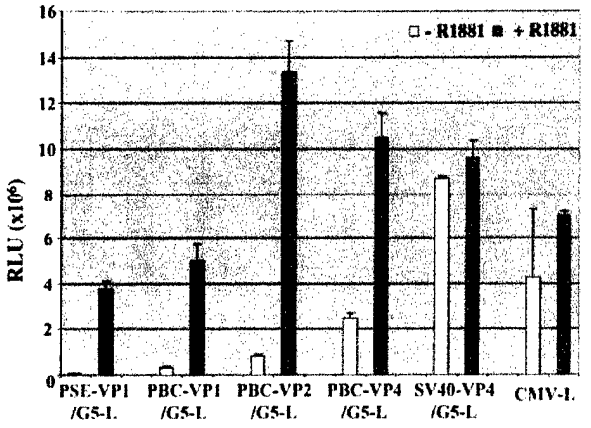

FIG. 4. Comparing different numbers of activation domains. We transfected LNCaP cells with G5-L and either GAL4-VP1, -VP2, or -VP4 expression vectors driven by the PSE or chimeric (PBC) PSA enhancer-promoter. SV40-VP4/G5-L and CMV-L serve as benchmarks. We adjusted the DNA concentrations so that the transfections contained comparable molar amounts of the FL gene.

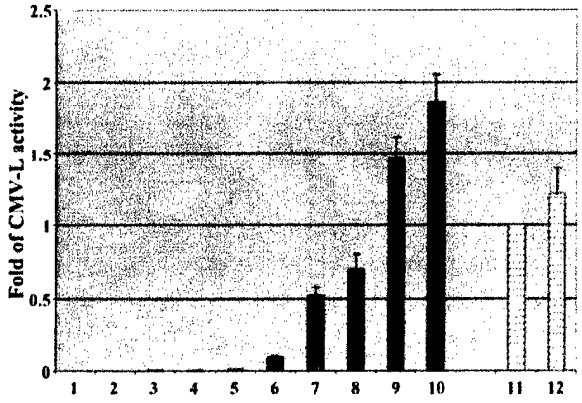

FIG. 5. The spectrum of activities generated by the TSTA system. We plotted results of the previous experimental combinations side-by-side for direct comparison. We normalized the measurements to CMV-L activity in the presence of R1881. CMV-L was assigned a value of 1. The samples are aligned by their activities: 1, PSE-L; 2, PSE-VP1/G1-L; 3, PBC-VP4/G1-L; 4, PBC-L; 5, PSE-VP1/G2-L; 6, PBC-VP4/G2-L; 7, PSE-VP1/G5-L; 8, PBC-VP1/G5-L; 9, PBC-VP4/G5-L; 10, PBC-VP2/G5-L; 11, CMV-L; 12, SV40-VP4/G5-L.

results (Fig. 6A) where PBC and SV40 expressed GAL4–VP2 at similar levels. However, PBC expression was androgen-dependent, whereas SV40 expression was not influenced by androgen.

We found that the TSTA system displayed activities comparable to the SV40 benchmark only in the prostate cancer cell lines, LNCaP and LAPC4 (> 90% and 75%, respectively; Fig. 6). In contrast, we found that the activities of the TSTA system relative to the benchmark were 0.2% in HepG cells, 0.7% in HeLa cells, and 1.5% in MCF-7 cells. In a system where AR was overexpressed, fAR-HeLa cells, the TSTA system elicited 2% the activity of our benchmark. The difference between HeLa and fAR HeLa was significant ($P = 0.4$).

The Effector and Reporter on the Same Plasmid

A single plasmid bearing both the effector and reporter greatly increased activity but maintained cell selectivity (Fig. 7). The construct, referred to as PBCVP2G5-L, contains a 3.5-kb PBC-VP2 *Not*I fragment inserted into the G5-L (Fig. 1D) in a "head-to-head" orientation, with 170 bp between G5 and the 5' end of the distal copy of the PSA core enhancer. Transfection of the single construct PBCVP2G5-L into LNCaP cells yielded an activated FL activity 10-fold higher than that seen with the same molar amount of the two-construct PBC-VP2/G5-L TSTA system. The single construct did not display as much activity relative to the benchmark in LAPC4 cells, possibly due to the reduced androgen dependency of LAPC4. Nevertheless, PBCVP2G5-L maintained tissue selectivity as illustrated by its low activity in HeLa, fAR-HeLa, HepG2, and MCF7 cells. When we cloned the PBC-VP2 *Not*I fragment in the "head-to-tail" orientation with G5-L to generate a single construct, we discovered that PBCVP2G5-L(R) displayed greatly reduced activity versus the head-to-head orientation (data not shown). We do not understand the cause of this effect.

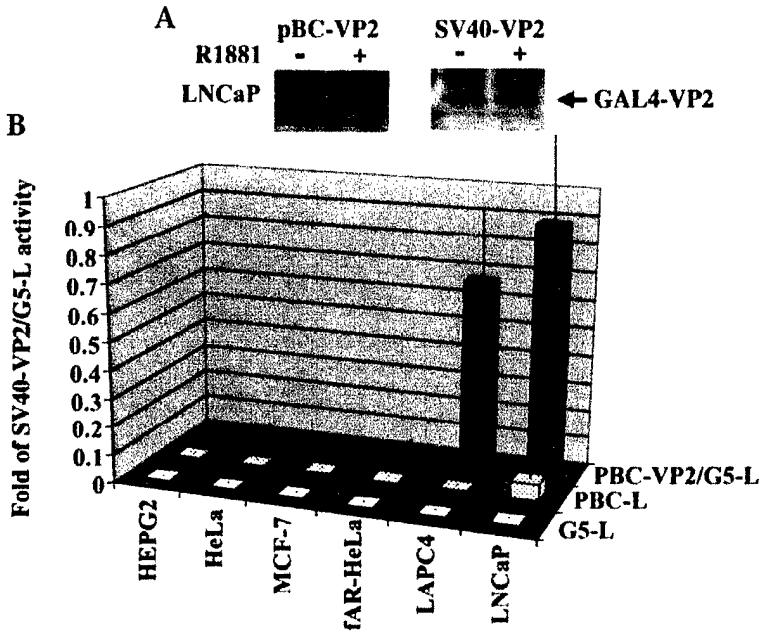

FIG. 6. Cell-specific expression and androgen inducibility of the TSTA system. (A) Immunoblot analyses demonstrating the expression of GAL4–VP2 from the optimized PBC-VP2 construct versus our benchmark SV40-VP2. We transfected LNCaP cells with PBC-VP2/G5-L or SV40-VP2/G5-L with or without androgen treatment. The samples were prepared, blotted, and probed with GAL4VP16 antibodies. (B) We seeded six human cell lines in six-well plates and transfected as described. The same molar amount of luciferase gene was transfected into all the cell types with a total DNA amount of 0.5 μg per well. We normalized all the RLU readings to the values obtained from the combination of SV40-VP2 and G5-L transfected into the same cell line. The SV40-VP2/G5-L value was set at 1 in the three-dimensional plot. We used PBC-L as a control for promoter specificity of the effector and measured the background by transfection of G5-L alone.

doi:10.1006/mthe.2002.0551, available online at http://www.idealibrary.com on IDEAL

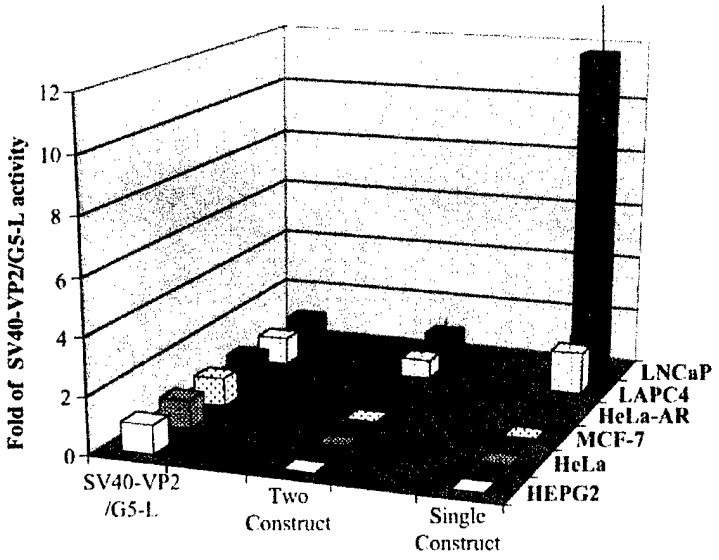

FIG. 7. Cell-specific expression of the single construct. We transfected six human cell lines with SV40-VP2/G5-L, PBC-VP2/G5-L, or the single construct. All the cells were transfected with the same molar amount of luciferase DNA. The cells were sampled, analyzed, and graphed as in Fig. 6, except we switched the axes on the cell lines and transfected plasmids to simplify the presentation.

Application of the Chimeric TSTA System to Imaging FL Reporter Gene Expression in Living Mice

We found that the chimeric TSTA system displays robust expression in imaging studies in live mice. To validate the potential of the modified TSTA for imaging, we determined whether the differences in activity could be reproduced qualitatively in an animal imaging system. A CCD camera converts bioluminescent photons to quantifiable electronic signals. The luminescence is recorded and graphically displayed by superimposing a colored topographic pseudoimage on a photograph of the animal. Previous studies had established that within the proper time frame, the RLU signals acquired by the camera are linear to exposure time and amount of FL activity as assayed by luminometry [32]. We transfected LNCaP cells or HeLa cells with our optimal TSTA constructs, treated them with R1881, and implanted the cells subcutaneously onto the dorsal surface of the mice. We separated the mice into four groups. Within each group we injected three types of transfected cells. To eliminate positional artifacts, we performed the experiments in triplicate; we rotated each group of cells through all three implantation sites. In group 1 (Fig. 8A), the G5-L negative control showed no detectable signal and the signal generated by PSE-L was barely above the background. In contrast the signal for the one-step vector PBC-L was evident and equal to 800 relative light units (RLU)/minute at the maximum intensity. When we analyzed the two-step system (Fig. 8B), signals of over 6500 RLU/minute were obtained with the optimal two-construct TSTA system.

The signals appeared to be both ligand- and cell-specific. HeLa cells transfected with PBC-VP2/G5-L (Fig. 8C) or LNCaP cells grown without R1881 did not display a signal above background (data not shown). We estimated the maximum signal from PBCVP2G5-L, the single construct, to be 55,000 RLU/minute, which is nearly 10-fold greater than the signal generated by the two-construct TSTA system (Fig. 8D). CMV-L exhibited a similar signal in both LNCaP (Fig. 8D) and HeLa cells (Fig. 8C).

Discussion

Use of the Chimeric TSTA System to Modulate Expression

We have modulated the activity of the TSTA system by introducing potent PSA enhancers and potent derivatives of GAL4–VP16. Remarkably, the largest increases in activity came not from increasing the potency of the PSA promoter but from either increasing the potency of the activator or by placing the TSTA components on a single plasmid. Increasing the number of activator-binding sites from G1 to G5 greatly amplifies the activity by 240- to 450-fold, depending on the activator expressed (PSE-VP1 or PBC-VP4; Fig. 3). Moreover, duplication of the activation domain from PBC-VP1 to PBC-VP2 resulted in a threefold enhancement of activity. These results reinforce the concept of synergistic activation of transcription and its use in varying the activity of an expression system.

We observed the most dramatic increase in activity by placing the TSTA system on a single plasmid. Comparison in LNCaP cells of the single construct, PBCVP2G5-L, with the combination constructs, PBC-VP2 and G5-L, revealed a 10-fold difference. The positioning of the two components on the same DNA molecule may generate a feed-forward loop, where GAL4–VP16 drives G5-L and raises its own expression level by binding upstream of PBC. Similar loops have been described [33].

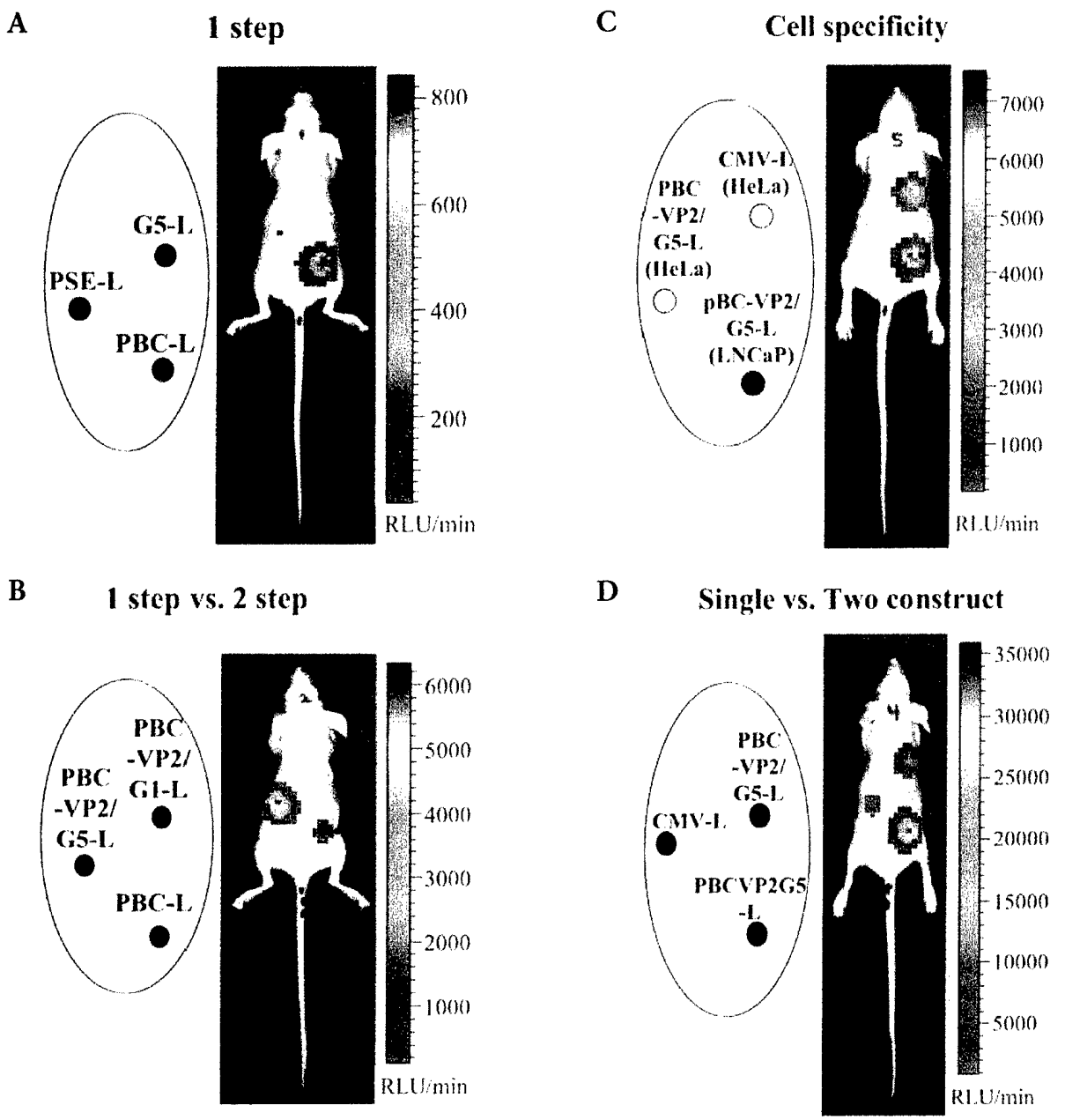

FIG. 8. Imaging of one-step and TSTA in living athymic nude mice. (A–D) Pictures shown in the figure are bioluminescent color images superimposed on the gray-scale mouse photographs. The color scale is in units of RLU/min and is to the right of each photo. Note that the scales vary among experiments. A map representing the dorsal surface of the mice is on the left; the circles denote the relative position of the three injection spots, with the transfected plasmids labeled over each circle. We also marked the needlepoints on the mouse with a red marker. A description of the group is shown on top of each panel and the acquisition time of the CCD camera for each image generated is in parentheses.

There are numerous combinations that could still be tested. The effects of the PSE-VP2 or -VP4 series have not been compared with PBC-VP2 and -VP4. Additionally, certain conditions, such as the R1881 concentration, have not been adjusted; this was performed in an earlier study [22]. However, the values will likely fall within the ranges we observed. The study has indicated that we have reached, or are close to, the limit of amplification using the present TSTA components.

Others have explored the concept of TSTA in imaging and gene therapy. The Fraser group used a TSTA system, which used a GFP effector, and achieved enhanced,

tissue-specific bioluminescent signals to study zebrafish development [29]. Segawa and colleagues combined the PSA wild-type enhancer-promoter with GAL4–VP16 for gene therapy in prostate cancer [21] and we recently used an early version of TSTA in imaging.

Remarkable progress has been reported by others, who have explored the optimization of prostate-specific promoters. For example, the prostate-specific PSA and human kallikrein-2 (K2) promoter/enhancers have been modified to generate potent androgen-responsive expression systems analogous to our chimeric enhancers [34,35]. A direct comparison of the studies is difficult because of differences in enhancers, reporters (GFP versus FL), minimal promoters, positive benchmarks (different CMV constructs), or methods of DNA transduction. We emphasize that our study was geared towards the same endpoint as the others, but we focused on increasing potency and signal flexibility for use in imaging and therapy. By using transient transfection assays we demonstrated the amplitude, titratability, and specificity of our system over an 800-fold range. We tested certain points within this range and they maintained the same approximate activities by a cooled CCD imaging approach. The strongest constructs repeatedly exceeded the activities of multiple benchmarks.

Activity, Inducibility, and Specificity

The current methodology prohibits us from drawing conclusions about the absolute degree of androgen inducibility. Basal expression increased as the activity of the system increased from the one-step to the most potent two-step constructs. We believe that much of the increase in basal expression is a consequence of incomplete depletion of steroids from the cultured cells. The argument is based on two observations. First, the basal activity of the PSA enhancer constructs in charcoal-stripped serum can be further reduced by addition of the anti-androgen casodex (unpublished data). Second, the small amount of residual androgen in charcoal-stripped medium will likely result in the same amount of activator being synthesized when comparing different GAL4–VP16 derivatives expressed from a similar promoter such as PBC. This point is supported by our result showing that the threefold increase in potency of activators, that is, PBC-VP1 versus PBC-VP2, is observed in both the presence and absence of R1881. Nevertheless, the system still displayed cell type specificity. Ultimately, the most rigorous test of true androgen responsiveness and tissue-specific expression will be to perform transgenic animal studies or to use viruses stably expressing the TSTA system to infect xenografts or other animal models; this is the current focus of our research.

Applications to *in Vivo* Imaging

The cooled CCD optical imaging belongs to a new generation of *in vivo* imaging technologies that use fluorescent or bioluminescent reporter genes to produce a signal from within a living animal. The CCD approach detects low levels of luminescence consistently and reproducibly from fur-covered animals without the need for an external light source [32,36].

Luciferase monitoring of transgene expression is still in its infancy and is limited to small animals due to significant absorption and scatter of visible light within the animal [32]. Positron emission tomography (PET) is a technology currently used in clinical settings [37–39]. PET uses molecular probes labeled with positron-emitting isotopes and produces dynamic signals measurable by a circular array of detectors. PET generates tomographic images reflecting the concentration and location of probes in a living subject of any size. Successful PET imaging has been performed with the herpes-simplex-virus-1 (HSV-1) thymidine kinase (TK) reporter gene expressed from a CMV enhancer [37,39]. TK uses ^{18}F-labeled ganciclovir/penciclovir to generate a signal primarily in cells expressing the reporter gene. However, for some applications PET may have a lower sensitivity than bioluminescence imaging [32]. A significant improvement in sensitivity, in order to image the least number of cells, is necessary to make reporter gene based PET methods viable for imaging prostate cancer progression in preclinical and clinical models. The modifications reported in our current system are aimed at improving a prostate-specific PET-based reporter gene methodology.

Extensions of the TSTA System

The TSTA system can be manipulated for use in targeting cancer in different ways. New cell- and promoter-specific regulatory elements can be introduced to further up- or downregulate expression [16]. Replacement of the VP16 activation domain with domains responsive to unique signals can be used to identify novel cellular signaling pathways. Furthermore, other prostate cancer promoters can be used and novel reporter or therapeutic genes can be added. These additions will increase the utility and regulatability of TSTA. Although androgen and AR are central to early prostate cancer progression, later stages of proliferation gradually use cross-talk among AR and signaling cascades including MAPK, PI3K, PKA, EGFR, IGFR, and TGF-β [31,40–43]. The concept of TSTA can be readily applied to understanding the ramifications and activity of these cellular pathways during cancer progression. The major advances of TSTA are its cell selectivity, activity, and robustness relative to cell-specific promoters. Its flexibility will permit widespread utility in cancer research.

Materials and Methods

Cell culture. We grew the human prostate cancer cell line LNCaP in RPMI 1640 supplemented with 10% fetal bovine serum (FBS) and 1% penicillin/streptomycin solution. We grew HeLa, fAR-HeLa [10], and the human hepatic line HepG cells (ATCC) in DMEM with 10% FBS and 1% penicillin/streptomycin. We grew the human prostate cancer line LAPC4

[31] in IMDM (GIBCO) with 10% FBS and 1% penicillin/streptomycin. Before transfection, we transferred the cells for 24 hours into medium that contains 5% charcoal stripped serum.

Plasmids. The baseline PSA promoter construct termed PSE and the chimeric PSE-BC (abbreviated here as PBC) are as described [15]. To construct pPSE-VP1, the *Hin*dIII-*Xba*I fragment was excised from pSV40-VP1 and inserted downstream of the 2.4-kb PSA promoter PSE. We generated the other effectors, PBC-VP1, PBC-VP2, and PBC-VP4, using similar strategies [15]. We constructed G1, G2, and G5-L as described [22]. We cloned the *Not*I fragment bearing the PBC promoter and GAL4–VP2 gene into the *Not*I site of G5-L, generating a single vector termed PBCVP2G5-L that contained both components of the TSTA system.

Cell transfection. On day 1, we plated LNCaP cells in 6-well plates in RPMI 1640 containing charcoal-stripped FBS. We performed transient transfections 24 hours later using Tfx-50 (Promega) with a lipid:DNA ratio of 4:1. Each transfection mixture contained 0.5 μg of the effector and reporter plasmids or reporter plasmid alone with pGL3B carrier DNA. Methylenetrienolone (R1881; NEN Life Science Products, Boston, MA) was added to the medium at a concentration of 10 nM/well 1 hour following transfection, and the cells were incubated for 48 hours. The cells were harvested and lysed using the passive lysis buffer provided in the assay kit for measuring FL activities (Dual-Reporter Luciferase Assay System, Promega). FL activities of 5% of the cell lysates with 100 μl of substrate D-luciferin were measured using a luminometer (Lumat 9507, Berthod Germany) with an integration time of 10 seconds.

Immunoblot analysis of GAL4–VP16 expression. LNCaP cells were grown in 10-cm dishes and transfected with select plasmids expressing the TSTA components. We harvested and lysed the treated cells using RIPA lysis buffer (10 mM Tris-HCl, 150 mM NaCl, 0.1% SDS, 1% DOC, 1 mM EDTA, and 1% NP40). We normalized extracts by protein concentration (Bio-Rad Dc protein assay kit) and the samples were fractionated on 4–15% gradient acrylamide gels (Bio-Rad) and subjected to immunoblot analysis with rabbit polyclonal antibodies generated against intact GAL4–VP16 [44].

In vivo studies. We treated transiently transfected LNCaP and HeLa cells with 10 μM R1881, harvested 40 hours post-transfection, and resuspended in phosphate buffered saline (PBS). We anesthetized female nu/nu mice with 40 μl ketamine-xylazine (4:1) solution. To allow time for tissue distribution, a solution of D-luciferin (Xenogen, CA) in PBS (200 ml, 15 mg/ml) was injected into the peritoneal cavity before implanting cells. After 5 minutes, 1×10^6 cells were suspended in 50 μl PBS, combined with 50 μl Matrigel (BD Biosciences, Bedford, MA), and injected subcutaneously onto the dorsal side of the mice. Each mouse bore injections at three sites. Twenty minutes after intraperitoneal injection of D-luciferin, we imaged the mice using a cooled CCD camera (Xenogen IVIS, Xenogen Corp., Alameda, CA). At the time of injection into animals, an aliquot of the cells was also analyzed for FL activity using a luminometer as described above. All studies were performed with full approval from the UCLA Animal Research Committee (ARC).

CCD imaging and quantitation. We placed the mice prone in a light-tight chamber and a gray-scale reference photograph was obtained under low-level illumination. We collected photons emitted from within the mouse and transmitted through tissue and integrated them for an acquisition time of 1 to 5 minutes. We obtained images and analyzed them using Living Image Software v4.02 A (Xenogen Corporation, Alameda, CA) v2.11 and Igor Image Analysis Software (Wavemetrics, Seattle, WA). We drew regions of interest (ROI) over the visible light signal to quantitate the light. We normalized the maximum RLU signals measured to acquisition time to obtain maximum RLU/minute. We calibrated the system as described [32].

Acknowledgments

This work is supported in part by NIH grants P50 CA86306 (S.S.G.), SAIRP R24 CA92865 (S.S.G.), DOD PC 991019 (M.C.), Department of Energy Contract DE-FC03-87ER60615 (S.S.G.), and CaP CURE (S.S.G., M.C.).

RECEIVED FOR PUBLICATION OCTOBER 26;
ACCEPTED DECEMBER 21, 2001.

References

1. Somia, N., and Verma, I. M. (2000). Gene therapy: trials and tribulations. *Nat. Rev. Genet.* **1**: 91–99.
2. Shalev, M., *et al.* (2001). Gene therapy for prostate cancer. *Urology* **57**: 8–16.
3. Anderson, W. F. (1998). Human gene therapy. *Nature* **392**: 25–30.
4. Taneja, S. S., Pang, S., Cohan, P., and Belldegrun, A. (1995). Gene therapy: principles and potential. *Cancer Surv.* **23**: 247–266
5. Rubinchik, S., *et al.* (2000). Adenoviral vector which delivers FasL-GFP fusion protein regulated by the tet-inducible expression system. *Gene Ther.* **7**: 875–885.
6. Cleutjens, K. B., *et al.* (1996). Two androgen response regions cooperate in steroid hormone regulated activity of the prostate-specific antigen promoter. *J. Biol. Chem.* **271**: 6379–6388.
7. Schuur, E. R., *et al.* (1996). Prostate-specific antigen expression is regulated by an upstream enhancer. *J. Biol. Chem.* **271**: 7043–7051.
8. Farmer, G., Connolly, E. S., Jr., Mocco, J., and Freedman, L. P. (2001). Molecular analysis of the prostate-specific antigen upstream gene enhancer. *Prostate* **46**: 76–85.
9. Pang, S., *et al.* (1995). Prostate tissue specificity of the prostate-specific antigen promoter isolated from a patient with prostate cancer. *Hum. Gene. Ther.* **6**: 1417–1426.
10. Huang, W., *et al.* (1999). Cooperative assembly of androgen receptor into a nucleoprotein complex that regulates the prostate-specific antigen enhancer. *J. Biol. Chem.* **274**: 25756–25768.
11. Yeung, F., *et al.* (2000). Regions of prostate-specific antigen (PSA) promoter confer androgen-independent expression of PSA in prostate cancer cells. *J. Biol. Chem.* **275**: 40846–40855.
12. Perez-Stable, C. M., Pozas, A., and Roos, B. A. (2000). A role for GATA transcription factors in the androgen regulation of the prostate-specific antigen gene enhancer. *Mol. Cell. Endocrinol.* **167**: 43–53.
13. Oettgen, P., *et al.* (2000). PDEF, a novel prostate epithelium-specific ets transcription factor, interacts with the androgen receptor and activates prostate-specific antigen gene expression. *J. Biol. Chem.* **275**: 1216–1225.
14. Murphy, E. P., *et al.* (2001). Involvement of the nuclear orphan receptor NURR1 in the regulation of corticotropin-releasing hormone expression and actions in human inflammatory arthritis. *Arthritis Rheum.* **44**: 782–793.
15. Wu, L., *et al.* (2001). Chimeric PSA enhancers exhibit augmented activity in prostate cancer gene therapy vectors. *Gene Ther.* **8**: 1416–1426.
16. Nettelbeck, D. M., Jerome, V., and Muller, R. (2000). Gene therapy: designer promoters for tumour targeting. *Trends Genet.* **16**: 174–181.
17. Sadowski, I., Ma, J., Triezenberg, S., and Ptashne, M. (1988). GAL4-VP16 is an unusually potent transcriptional activator. *Nature* **335**: 563–564.
18. Carey, M., Lin, Y. S., Green, M. R., and Ptashne, M. (1990). A mechanism for synergistic activation of a mammalian gene by GAL4 derivatives. *Nature* **345**: 361–364.
19. Fischer, J. A., Giniger, E., Maniatis, T., and Ptasne, M. (1998). GAL4 activates transcription in Drosophilia. *Nature* **332**: 853–856.
20. Brand, A. H., and Perrimon, N. (1993). Targeted gene expression as a means of altering cell fates and generating dominant phenotypes. *Development* **118**: 401–415.
21. Segawa, T., *et al.* (1998). Prostate-specific amplification of expanded polyglutamine expression: a novel approach for cancer gene therapy. *Cancer Res.* **58**: 2282–2287.
22. Iyer, M., *et al.* (2001). Two-step transcriptional amplification as a method for imaging reporter gene expression using weak promoters. *Proc. Natl. Acad. Sci. USA* **98**: 14595–14600.
23. Gambhir, S. S., *et al.* (2000). Imaging transgene expression with radionuclide imaging technologies. *Neoplasia* **2**: 118–138.
24. Auclerc, G., *et al.* (2000). Management of advanced prostate cancer. *Oncologist* **5**: 36–44.
25. Sadar, M. D., Hussain, M., and Bruchovsky, N. (1999). Prostate cancer: molecular biology of early progression to androgen independence. *Endocr. Relat. Cancer* **6**: 487–502.
26. Lee, C., *et al.* (1995). Regulation of proliferation and production of prostate-specific antigen in androgen-sensitive prostatic cancer cells, LNCaP, by dihydrotestosterone. *Endocrinology* **136**: 796–803.
27. Joly-Pharaboz, M. O., *et al.* (1995). Androgens inhibit the proliferation of a variant of the human prostate cancer cell line LNCaP. *J. Steroid Biochem. Mol. Biol.* **55**: 67–76.
28. Gill, G., and Ptashne, M. (1988). Negative effect of the transcriptional activator GAL4. *Nature* **334**: 721–724.
29. Koster, R. W., and Fraser, S. E. (2001). Tracing transgene expression in living zebrafish embryos. *Dev. Biol.* **233**: 329–346.
30. Emami, K. H., and Carey, M. (1992). A synergistic increase in potency of a multimerized VP16 transcriptional activation domain. *EMBO J.* **11**: 5005–5012.
31. Craft, N., Shostak, Y., Carey, M., and Sawyers, C. L. (1999). A mechanism for hormone-independent prostate cancer through modulation of androgen receptor signaling by the HER-2/neu tyrosine kinase. *Nat. Med.* **5**: 280–285.
32. Wu, J. C., Sundaresan, G., Iyer, M., and Gambhir, S. S. (2001). Noninvasive optical imaging of firefly luciferase reporter gene expression in skeletal muscles of living mice. *Mol. Ther.* **4**: 297–306.
33. Nettelbeck, D. M., Jerome, V., and Muller, R. (1998). A strategy for enhancing the transcriptional activity of weak cell type- specific promoters. *Gene Ther.* **5**: 1656–1664.
34. Latham, J. P., Searle, P. F., Mautner, V., and James, N. D. (2000). Prostate-specific antigen promoter/enhancer driven gene therapy for prostate cancer: construction and

doi:10.1006/mthe.2002.0551, available online at http://www.idealibrary.com on IDEAL

testing of a tissue-specific adenovirus vector. *Cancer Res.* **60**: 334–341.
35. Xie, X., *et al.* (2001). Robust prostate-specific expression for targeted gene therapy based on the human kallikrein 2 promoter. *Hum. Gene Ther.* **12**: 549–561.
36. Honigman, A., *et al.* (2001). Imaging transgene expression in live animals. *Mol. Ther.* **4**: 239–249.
37. Gambhir, S. S., *et al.* (1999). Imaging adenoviral-directed reporter gene expression in living animals with positron emission tomography. *Proc. Natl. Acad. Sci. USA* **96**: 2333–2338.
38. Herschman, H. R., *et al.* (2000). Seeing is believing: non-invasive, quantitative and repetitive imaging of reporter gene expression in living animals, using positron emission tomography. *J. Neurosci. Res.* **59**: 699–705.
39. Gambhir, S. S., *et al.* (1998). Imaging of adenoviral-directed herpes simplex virus type 1 thymidine kinase reporter gene expression in mice with radiolabeled ganciclovir. *J. Nucl. Med.* **39**: 2003–2011.
40. Putz, T., *et al.* (1999). Epidermal growth factor (EGF) receptor blockade inhibits the action of EGF, insulin-like growth factor I, and a protein kinase A activator on the mitogen-activated protein kinase pathway in prostate cancer cell lines. *Cancer Res.* **59**: 227–233.
41. Gioeli, D., *et al.* (1999). Activation of mitogen-activated protein kinase associated with prostate cancer progression. *Cancer Res.* **59**: 279–284.
42. Lin, J., Adam, R. M., Santiestevan, E., and Freeman, M. R. (1999). The phosphatidylinositol 3'-kinase pathway is a dominant growth factor-activated cell survival pathway in LNCaP human prostate carcinoma cells. *Cancer Res.* **59**: 2891–2897.
43. Sadar, M. D. (1999). Androgen-independent induction of prostate-specific antigen gene expression via cross-talk between the androgen receptor and protein kinase A signal transduction pathways. *J. Biol. Chem.* **274**: 7777–7783.
44. Carey, M., Leatherwood, J., and Ptashne, M. (1990). A potent GAL4 derivative activates transcription at a distance in vitro. *Science* **247**: 710–712.

HUMAN GENE THERAPY 13:000–000 (May 1, 2002)

IN PRESS

Optimizing Prostate Cancer Suicide Gene Therapy Using Herpes Simplex Virus Thymidine Kinase Active Site Variants

ALLAN J. PANTUCK,[1] JAMIE MATHERLY,[1] AMNON ZISMAN,[1] DAVID NGUYEN,[1] FRANK BERGER,[2] SANJIV S. GAMBHIR,[2] MARGARET E. BLACK,[3,4] ARIE BELLDEGRUN,[1] and LILY WU[1]

ABSTRACT

The herpes simplex virus (HSV) thymidine kinase gene (tk) forms the basis of a widely used strategy for suicide gene therapy. A library of HSV thymidine kinase enzyme (TK) active site mutants having different affinities for guanosine analog prodrugs was developed. We sought to determine the optimal combination of tk variant and prodrug specifically for prostate cancer gene therapy, using *in vitro* and *in vivo* studies of adenovirally infected CL1, DU-145, and LNCaP tumor lines carrying wild-type tk, tk30, tk75, and sr39tk mutants expressed by a strong, constitutive cytomegalovirus promoter and treated with ganciclovir and acyclovir. *In vitro* experiments involving prostate cancer (CaP) cell line infection were carried out with a broad range of prodrug concentrations, and cell killing was determined by limiting dilution (colony-forming), MTT, and propidium iodide assays. *In vivo* studies based on CL1-GFP xenograft experiments were carried out to examine the ability of each TK variant to prevent tumor formation and to inhibit tumor growth and development of metastases in established orthotopic and subcutaneous tumors in SCID mice. Both *in vitro* and *in vivo* studies suggest improved killing with the sr39tk variant. Thus, the results suggest that the use of SR39 in future trials of prostate cancer tk suicide gene therapy may be beneficial.

OVERVIEW SUMMARY

Gene therapy holds promise as an alternative or adjuvant treatment for advanced, aggressive stages of cancer, such as prostatic carcinoma, for which no curative options are available. Herpes simplex virus 1 thymidine kinase enzyme (TK)-mediated suicide gene therapy is a widely used strategy in experimental models and clinical trials. One approach that could enhance the cytotoxic activity of TK is to use variant enzymes that have been reengineered with increased affinity for prodrugs as compared with thymidine. In this study, we evaluated the therapeutic efficacy of a panel of adenoviral vectors expressing the tk active site variants with the acyclovir and ganciclovir prodrugs in prostate cancer cell lines and tumor xenografts. Our ultimate goal is to improve the therapeutic efficacy of tk suicide gene therapy for prostate cancer.

INTRODUCTION

PATIENTS WITH advanced prostate cancer have a poor prognosis, and currently available treatment options for advanced prostate cancer are limited and lack curative potential. Gene therapy represents a powerful new alternative for cancer treatment. Several prototypes of gene therapy protocols have been investigated in preclinical studies for the treatment of prostate cancer, including gene replacement or antisense strategies to restore normal growth control (Eastham *et al.*, 1995; Dorai *et al.*, 1997; Morelli *et al.*, 1997), insertion of genes to stimulate the immune system (Vieweg *et al.*, 1994; Sokoloff *et al.*, 1996; Simons *et al.*, 1999; Belldegrun *et al.*, 2001), and delivery of genes that cause the activation of a prodrug that induces selective cytoxicity and destruction of tumor cells (Eastham *et al.*, 1996; Blackburn *et al.*, 1998).

AU1

Viral transduction of the herpes simplex virus type 1 (HSV-

[1]Department of Urology, University of California School of Medicine, Los Angeles, CA 90095.
[2]Crump Institute for Molecular Imaging, University of California School of Medicine, Los Angeles, CA 90095.
[3]Department of Pharmaceutical Sciences, Washington State University, Pullman, WA 99164.
[4]Chiroscience R & D, Bothell, WA 98021.

1) thymidine kinase gene (tk), followed by systemic delivery of ganciclovir (GCV), is a cytotoxic gene therapy approach that is considered a potential strategy for prostate cancer treatment (Hall *et al.*, 1997; Herman *et al.*, 1999; Hassan *et al.*, 2000). In contrast to human thymidine kinase (TK), which phosphorylates acycloguanosines only minimally, HSV-1 TK has a relaxed substrate specificity for other nucleoside analogs, and can phosphorylate a variety of acycloguanosine and uracil derivatives, including the acyclic analogs of deoxyguanosine such as acyclovir (ACV) and GCV. The cytotoxic effect of GCV is due to its incorporation into DNA by a process involving several steps, beginning with its conversion by the TK enzyme to GCV monophosphate. The monophosphorylated GCV undergoes further phosphorylation by endogenous cellular kinases into the corresponding nucleoside triphosphate, which is incorporated into cellular DNA and prevents DNA synthesis, which ultimately results in cell death by several proposed mechanisms (Wallace *et al.*, 1996; Rubsam *et al.*, 1999; Mesnil and Yamasaki, 2000).

New tk variants have been developed to improve the potency of antitumor effects. These variants were generated by random mutagenesis of the binding site amino acids, and selected for increased affinity for the prodrugs GCV and ACV, as compared with thymidine (Black *et al.*, 1996, 2001). We compared the therapeutic efficacy of a panel of adenoviral (Ad) vectors expressing the tk active site variants with wild-type tk in terms of processing ACV and GCV prodrug in prostate cancer cell lines and tumor xenografts. Our goal is to improve the therapeutic efficacy of the tk suicide gene therapy scheme for prostate cancer.

AU2

MATERIALS AND METHODS

Cell culture and viral vectors

The human prostate cancer cell line LNCaP was provided by the American Type Culture Collection (Rockville, MD). The human prostate cancer cell line CL1 was derived as previously described (Patel *et al.*, 2000). LNCaP cells were maintained in RPMI 1640 medium with 10% fetal bovine serum, glutamine, and antibiotics (penicillin [50 IU/ml] and streptomycin [50 μg/ml]). CL1 cells were maintained in RPMI 1640 medium with 10% charcoal-stripped serum, glutamine, and antibiotics. As previously described, CL1 cells were transfected with a green fluorescent protein (GFP) marker (Patel *et al.*, 2000). The established CL1-GFP cell line contained 99.9% GFP-expressing cells, as determined by flow cytometry.

First-generation E1-deleted Ad vectors containing wild-type thymidine kinase (Ad-CMV-HSV1-tk); the tk mutants sr39 (Ad-CMV-HSV1-sr39tk), tk30 (Ad-CMV-HSV1-tk30), and tk75 (Ad-CMV-HSV1-tk75); and control Ad containing either green fluorescent protein or β-galactosidase genes were generated, purified, and characterized as previously described (Gambhir *et al.*, 1999, 2000; Tan *et al.*, 1999).

Southern and Western blot analyses

A modified Hirt DNA isolation procedure (Tan *et al.* 1999) was used to obtain low molecular weight DNA from cells 24 hr after adenovector infection. Hirt DNA from 10^7 infected CL1 cells was analyzed by Southern blotting, using a nonradioactive digoxigenin-labeled 1.9-kb HSV-TK DNA probe (Roche, Indianapolis, IN). Transferred DNA on nylon membranes (Hybond; Amersham, Arlington Heights, IL) was detected by colorimetric conversion of nitroblue tetrazolium (NBT) and 5-bromo-4-chloro-3-indolyl phosphate (BCIP). All procedures were performed according to the manufacturer protocols.

TK-expressing or control adenovirus-infected cells were lysed in a homogenization buffer containing pepstatin (1.45 m*M*), leupeptin (2.1 m*M*), dithiothreitol (DTT), TEA-HCl (50 m*M*), and EDTA/EGTA (0.1 m*M*). Total protein (5–20 μg) was loaded in Laemmli buffer onto a 7.5% polyacrylamide gel. The proteins were transferred to nitrocellulose membranes for 1 hr, using a Mini Trans blot electrophoretic transfer cell (Bio-Rad, Hercules, CA). The membrane was blocked overnight in phosphate-buffered saline (PBS)–0.05% Tween 20–5% nonfat dry milk overnight at 4°C. After two washes in PBS–0.005% Tween 20, TK polyclonal serum (generously provided by M. Black, Department of Pharmaceutical Sciences, Washington State University, Pullman, WA) at a dilution of 1:5000 was added for 1.5 hr. After another three washes, secondary antibody was added for 1.5 hr. Using an enhanced chemiluminescence kit (Amersham Life Science, Piscataway, NJ), the membrane was developed on Kodak (Rochester, NY) film in a darkroom.

Cytotoxicity assays

Colony formation assay. Cells were infected at a multiplicity of infection (MOI) of 1, using tk variant or control Ad in 60-mm plates. Cells were trypsinized and replated into 12-well plates at a concentration of 100,000 cells/well at 24 hr postinfection. GCV or ACV was added to a final concentration of GCV ranging from 0.01 to 10 μM, and ACV ranging from 0.3 to 300 μM. After 4 days of prodrug exposure, the colony-forming efficiency of cell lines was measured by seeding cells at aliquots ranging from 1:10 to 1:500 in 60-mm petri culture dishes in prodrug-free media. After incubation for 10–14 days, cells were fixed with 80% alcohol for 30 min, and stained with 1% crystal violet solution in PBS. The visualized cell colonies were counted and compared.

MTT colorimetric assay. Subconfluent cells in 10-cm plates were infected with E1-deleted Ad containing the wild-type or mutant tk gene under the control of a cytomegalovirus (CMV) promoter at an MOI of 1. After 24 hr, cells were trypsinized, washed, centrifuged, and replated in triplicate at 10^4 cells/well in 24-well plates, with dose-escalating concentrations of prodrug added to each well. After 7 days, a 50-μl/well concentration of 10× stock 3-(4,5 dimethylthiazole-2-yl)-2,5-diphenyltetrazolium bromide (MTT) was added and allowed to incubate for 4 hr. Cells were lysed with 0.04 *M* HCl in isopropanol, and shaken for 10 min to dislodge adherent cells and disrupt clumps of formazan blue crystals. Cells (200 μl from each well) were transferred to a 96-well plate, and absorbance was measured at 595 nm with a microplate reader. A standard curve was generated with varying concentrations of untreated cells.

Propidium iodide assay for apoptosis

Treated cells were harvested, fixed, and subjected to propidium iodide (PI) staining and flow cytometry analysis for apoptosis. The cells were treated as in the MTT assay (described above), and after 5–7 days of drug exposure were harvested into

fluorescence-activated cell sorting (FACS) tubes (Fisher Scientific, Pittsburgh, PA), using gentle repeated irrigation with Dulbecco's PBS (GIBCO-BRL Life Technologies, Frederick, MD) containing 0.05% EDTA (Biofluids, Rockville, MD). The cells were washed twice with PBS and fixed for 30 min in 70% ethanol (Gold Shield Chemical, Hayward, CA) at −20°C, and subjected to PI staining. PI solution (100 μl, 50 μg/ml; Roche) containing RNase A1 (50 μg/ml) was added to each tube and incubated for 30 min at 37°C in a darkroom, and then the volume brought to 1.0 ml by adding 0.9 ml of PBS. The cells were subjected to flow cytometric analysis, using the Coulter (Miami Lakes, FL) system II and Epics software version 3.0. The parameter settings were optimized at the beginning of the study and kept constant through subsequent analyses.

Animal studies

Male 6- to 8 week-old severely compromised immunodeficient (SCID; CB.17 *scid/scid*) mice were obtained from the breeding program at the University of California at Los Angeles (UCLA), under a protocol approved by the UCLA Chancellor's Animal Research Committee. All animals were anesthetized with ketamine and xylazine before survival surgery and inoculation with cancer cells. The flanks of five SCID mice per treatment group were injected subcutaneously by 27-gauge needle with either 5×10^4 cells resuspended in 5 μl of RPMI 1640 into the accessory sex gland, or with 5×10^6 cells resuspended in 100 μl of RPMI 1640. For orthotopic, intraprostatic injection, a small 1-cm vertical midline incision in the lower abdomen was dissected into the peritoneum. Using the seminal vesicles as an anatomic landmark, the prostate was exposed. Cells were injected into the dorsal prostate lobes under the prostatic capsule, and then the abdominal wall and skin were closed with fine surgical sutures. For tumor prevention studies, cells were grown in 10-cm plates to 80% confluency, medium was removed, and the cells were infected with each tk or control adenovirus at an MOI of 1. Cells were harvested and injected into animals 24 hr postinfection, and treatment commenced the following day with GCV at 20 mg/kg by daily intraperitoneal or tail vein injection for a total of 6 days. In the established tumor model, injection of tk-expressing Ad (a total of 3×10^9 infectious units [PFU] into three sites on three separate days) began when subcutaneous tumors reached a diameter of 5 mm. Three-dimensional tumor growth was measured twice weekly, using calipers.

Animals were killed when their performance status was noted to deteriorate or when tumor diameters reached 15 mm. Tumor invasion was examined grossly by necroscopy, and histologically by evaluation of formalin-fixed, paraffin-embedded sections obtained from the primary tumor and multiple organs, lymph nodes, and bones, which were mounted and stained with hematoxylin and eosin. Micrometastasis was detected by fluorescence microscopy of GFP-positive cells. Fresh tumors and organ samples were snap frozen in isopentane and dry ice, embedded in O.C.T. medium for cryostat sections of 5 μm, and examined with a fluorescence microscope (Carl Zeiss, Thornwood, NY) with an adjustable camera with 400ASA color film (Kodak).

Flow cytometry analysis

To quantify metastasis, a portion of liver from each mouse was enzymatically digested and subjected to FACS analysis to determine the percentage of GFP-positive cells. The right hepatic lobe was excised, diced into small fragments, and enzymatically digested by gentle shaking in sterile RPMI medium containing collagenase type I (200 U/ml), DNase type I (250 μg/ml) (Sigma, St. Louis, MO). After Ficoll-Hypaque density gradient centrifugation (LSM; Organon Teknica, Durham, NC), the single-cell suspension was washed twice and resuspended in 0.5 ml of assay buffer. Fluorescence was analyzed on a FACScan II flow cytometer (Becton Dickinson Immunocytometry Systems, Mountain View, CA), and 5000–30,000 events were acquired for each sample, using FACScan research software. GFP-expressing tumors were used as positive controls, and uninfected livers as negative controls, to delineate the unstained/autofluorescent population. Events registered outside this trace were scored as positive, and the percentage of positive events was calculated.

CL1 cells stably expressing the sr39tk gene

To better understand the efficacy and limitations of gene therapy, and to begin to understand whether lack of *in vivo* tumor regression is due to vector delivery, transgene expression, or drug delivery, we investigated the feasibility of using positron emission tomography (PET) to image sr39tk expression in our prostate cancer xenograft model. CL1 cells were stably transfected with the sr39tk gene for the purpose of PET scanning to demonstrate tumor imaging, based on TK conversion of a radiolabeled penciclovir molecule into a trapped, metabolic product. Transfection was performed using Effectene (Qiagen, Chatsworth, CA). CL1 cells were grown until they were 70% confluent, and then transfected with 5 μg of plasmid DNA (pcDNA3.1/pCMV-sr39tk) on a 100-mm dish. After transfection (48 hr), the cells were selected with G418 (400 μg/ml) for 4 weeks. Selection continued for another 4 weeks at a G418 concentration of 800 μg/ml, but by this time most of the cells were resistant to the antibiotic. Stable TK expression by CL1-sr39tk cells was confirmed by Western blot analysis for TK protein and TK enzyme activity assay.

TK-mediated micro-PET

Male 6- to 8-week-old SCID (CB.17 *scid/scid*) mice were obtained from the breeding program at UCLA, with a protocol approved by the UCLA Chancellor's Animal Research Committee. The right flanks of mice were injected subcutaneously by 27-guage needle with 5×10^6 CL1-sr39tk cells resuspended in 100 μl RPMI 1640, and an equivalent number of CL1 cells was injected into the left flanks of the SCID mice. Mice were anesthetized as described previously before injection of tracer. Mice with tumors were serially imaged with FDG (fluorodeoxyglucose) and FHBG (a side chain-fluorinated penciclovir) tracers. Once tumors were palpable, mice were injected with 200–300 μCi of radiolabeled tracer, placed in a spread supine position, and scanned with the micro-PET (Gambhir *et al.*, 2000). Scanning was performed 60–90 min after tracer injection, to allow for clearance of background activity before starting image acquisition. Scanning was performed with the long axis of the mouse parallel to the long axis of the scanner, with the mouse in a prone position. Scanning conditions were identical to those previously described (MacLaren *et al.*, 1999). Acquisition time was 56 min, 8 min per position, with seven bed positions. Images were reconstructed with filter-back pro-

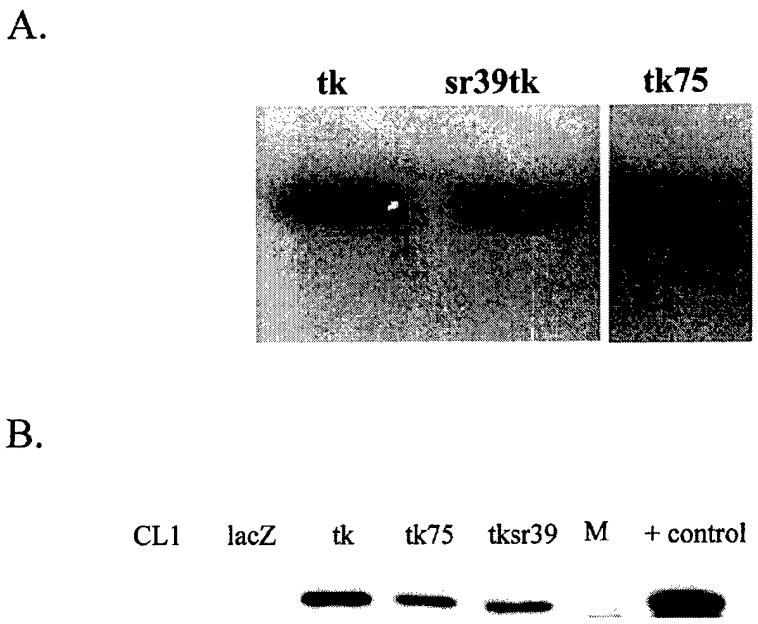

FIG. 1. Analysis of transduced viral gene and TK protein expression in infected cells. (**A**) Southern blot analysis of low molecular weight DNA from infected CL1 cells. Cells were infected at an MOI of 1 with the respective tk-expressing Ad. Hirt DNA isolated from 10^7 cells was subjected to restriction digestion, Southern blot transfer, and detection by the digoxigenin-labeled TK probe. Similar levels of tk gene were delivered to CL1 cells. (**B**) Western blot assay of infected CL1 cells. CL1 cells were infected at an MO1 of 1, and 10 μg of protein extract from uninfected or control Ad-infected or tk-expressing Ad-infected cells was loaded onto each lane. TK protein was visualized by a polyclonal antibody. "M" represents a marker lane, and "+ control" represents a sample from 293 cells infected with wild-type tk-expressing Ad.

jection and an iterative three-dimensional technique (Qi *et al.*, 1998), with an isotropic image resolution of 1.8 mm and a volumetric resolution of approximately 8 mm^3.

RESULTS

Standardization of viral infections

Studies by others (Gambhir *et al.*, 2000) have suggested that the amount of TK expression is related to the degree of prodrug sensitivity. A valid comparison between the effects of different mutant tk genes therefore requires standardization of protein concentrations. To verify that any observed differences between the prodrug-mediated cell killing for each tk mutant were not due to differences in gene delivery or gene expression, accurate viral titration and Southern and Western blot assays were performed for each infectant to quantify enzyme expression at the DNA and protein levels. Southern blotting of intracellular low molecular weight DNA to detect tk DNA (Fig. 1A) and TK protein Western blotting (Fig. 1B) were performed. There were no major differences between the amount of HSV-TK DNA or protein for tumor cells infected with equivalent dosages of the vectors containing the wild-type and tk variants. Thus, any enhanced killing was not due to overexpression.

F1

In vitro *prodrug sensitivity assays*

To evaluate the sensitivity of CL1 cells expressing the various TK variants to prodrug-mediated killing, tumor cells were cultured with increasing concentrations of GCV or ACV. The sensitivity of each TK variant to GCV or ACV was determined by three different cytoxicity assays, measuring both short- and long-term cell viability. Short-term cytotoxicity was evaluated by MTT and PI assays, whereas longer term cellular viability was measured by a colony formation assay. CL1 cells were infected with a viral vector expressing each tk variant, and were then assayed for their sensitivity to GCV or ACV. The results of a representative panel of cytotoxicity assays for the mutants and wild-type tk, along with a vector control for GCV and ACV, are shown in Figs. 2A–D and 3A–C, respectively.

F2&3

Because of the intrinsic differences of the three cytotoxicity assays, the precise measurements of viability and cell survival are not exactly the same. The results of the three assays complement each other and illustrate the same order of treatment efficacy among the wild-type and variant tk-expressing Ad. A colony-forming assay evaluated long-term survival with a more stringent requirement for cell replication. Thus, a more drastic impact of treatment was observed with colony-forming assays than with the short-term assays. The short-term assays (MTT and PI) evaluated cell damage incurred at one time point 5 days after prodrug treatment. Moreover, PI flow cytometry appeared to be the least sensitive of the three assays to detect cell damage. As illustrated in Fig. 2, GCV is a potent prodrug, as the LD_{50} for wild-type or sr39tk-expressing CL1 cells is 0.1 μM (Fig. 2A–C). The degrees of sensitivity for GCV of wild-type tk and sr39tk were similar, and both were only slightly higher than tk75, but dramatically higher than tk30 (Fig. 2).

As evaluated by short-term MTT assay, the LD_{50} of sr39tk-

expressing CL1 cells is 3 μM ACV, as compared with wild-type tk, which is 10-fold higher at 30 μM, and tk75, which is intermediate in potency at ~15 μM ACV (Fig. 3C). When comparing the results of ACV and GCV, however, equivalent killing was achieved with a 100-fold lower concentration of GCV compared with ACV. There was a strong correlation between the results of the three cytotoxicity assays. Assays were repeated several times, with similar results. These results were reproduced with a similar cytotoxicity profile in DU-145 cells, an androgen-independent prostate cancer line, and LNCaP cells, an androgen-responsive prostate cancer line (Fig. 4A and B). The same trend favoring sr39tk was also seen when the MTT assay was repeated with the HeLa cell line (data not shown). The results of early experimental data showing decreased cytotoxicity for tk30, compared with wild-type tk, precluded its use in further analysis.

F4

In vivo assays of tumor xenografts

Tumor prevention. CL1 cells that were infected *ex vivo* with wild-type and variant tk-expressing Ad were injected orthotopically into SCID mice. The CL1 xenograft model is a well-established, reproducible model with a well-known time course for local tumor formation, time course and pattern of metastasis, and time to death or sacrifice (Patel *et al.*, 2000). Untreated CL1 cells and an Ad carrying the β-galactosidase gene were used as negative control groups in parallel. The time course to both palpable tumor formation and death were doubled in treatment versus control groups (data not shown). The results for wild-type tk- and tk75-treated cohorts were similar, whereas there was an approximately 10% reduction in time to death or sacrifice for sr39tk versus wild type (data not shown). At the time of sacrifice, primary tumors and organs were collected for evaluation of tumor metastatic spread. The harvested organs were evaluated by conventional and fluorescence microscopy to qualitatively detect CL1-GFP metastasis (Fig. 5A). An attempt was made to assess metastatic burden more quantitatively by FACS analysis of the percentage of GFP-expressing cells in single-cell suspensions of treated and control livers. When comparing the untreated CL1-GFP group with the vector control group, wild-type tk decreased the hepatic metastatic tumor burden of positive green fluorescent cells, in the tissue analyzed, from 30 to 15% (Fig. 5B). Mice injected with sr39tk Ad-infected CL1-GFP cells showed an additional decrease in tumor burden to as low as <1% of total hepatic cells measured.

F5

Inhibition of established tumor progression. Subcutaneous CL1 tumors were established and allowed to grow to a tumor diameter of 5 mm before initiating treatment. Thereafter, mice were treated with two weekly intratumoral injections of Ad expressing wild-type or variant tk and six consecutive daily intraperitoneal injections of GCV (20 mg/kg). By 21 days after the treatment start date, the mean tumor diameter of the control, wild-type tk, tk75, and sr39tk groups was 11.2, 10.5, 9.5, and 6.5 mm, respectively. Although no tk mutant demonstrated complete eradication of tumor or improvement in overall survival, mice treated with sr39tk-expressing Ad showed a 63% reduction in tumor growth during the period of active treatment as compared with wild-type tk. We postulate that a limitation to more effective tumor eradication in this treatment strategy, using tk-expressing Ad, might lie in the difficulty of achieving adequate or even distribution after intratumoral injection of Ad. A sensitive and noninvasive method is needed to monitor transgene expression *in vivo*. Thus, we proceeded to evaluate the utility of micro-PET in our prostate cancer therapy strategy.

Micro-PET imaging of sr39 tk-expressing prostate cancer xenograft

It is convenient that the therapy tk gene can also serve as a PET reporter gene. CL1 tumors are aggressive, anaplastic, highly proliferative prostate cancer tumors. Consequently, both CL1 and CL1-sr39tk tumors are easily imaged by micro-PET, using the 2-^{18}F-fluoro-2-deoxyglucose (FDG) tracer, which is an analog of glucose metabolism (Fig. 6A). The same mouse was imaged with FHBG, which is an ^{18}F-labeled penciclovir (PCV) derivative. Cells containing the tk gene can phosphorylate FHBG, converting it into a trapped metabolic product that can be imaged by micro-PET. CL1-sr39tk but not CL1 tumors were easily visualized by FHBG micro-PET (Fig. 6B).

F6

DISCUSSION

Prostate cancer is currently the most frequently diagnosed malignancy and the second leading cause of cancer-related deaths in American men (Landis *et al.*, 1999). Once disease advances to metastasis, few treatment options exist, and none have curative potential. Recombinant DNA technology and the ability to manipulate DNA sequences, combined with techniques to transfer these sequences into mammalian cells, offer an alternative treatment approach in the form of gene therapy. Although still limited by a variety of technical problems, gene therapy, with its ultimate goal of efficient and targeted delivery of gene products that have significant anticancer activity, provides a powerful new concept for cancer treatment.

Approximately one-quarter of ongoing clinical trials are based on cytoreductive "suicide gene therapy" approaches (Herman *et al.*, 1999). Thus far, the HSV-TK/GCV system is the most extensively tested in cell culture, animal models, and clinical trials. Current clinical trial protocols of tk suicide gene therapy for prostate cancer include one based on direct intraprostatic injection of an Ad containing the tk gene, followed by intravenous administration of GCV (Shalev *et al.*, 2000). Adenovirus-delivered HSV-tk + GCV is also being evaluated in a phase I clinical trial at the Mount Sinai School of Medicine (New York, NY) in patients with clinically localized prostate cancer before radical prostatectomy (Hassan *et al.*, 2000). Overall, the HSV-tk/GCV regimen appears to be safe, even for multiple and repeated injections. These early trials will provide valuable information about the toxicity, the optimal techniques for intraprostatic injection, the effects on the prostate and prostate cancer tissue, and patterns of serum PSA response. However, long-term efficacy remains to be elucidated.

Efforts to improve the results of the tk suicide gene system by enhancing tumor cell killing without increasing prodrug-mediated toxicity in normal cells have been reported, with the creation of novel HSV-tk gene mutants that have increased specificity for phosphorylating GCV and/or ACV. From a library of more than 1 million variant tk genes created (Black *et al.*, 1996), several of them have been reported to have alterations in sub-

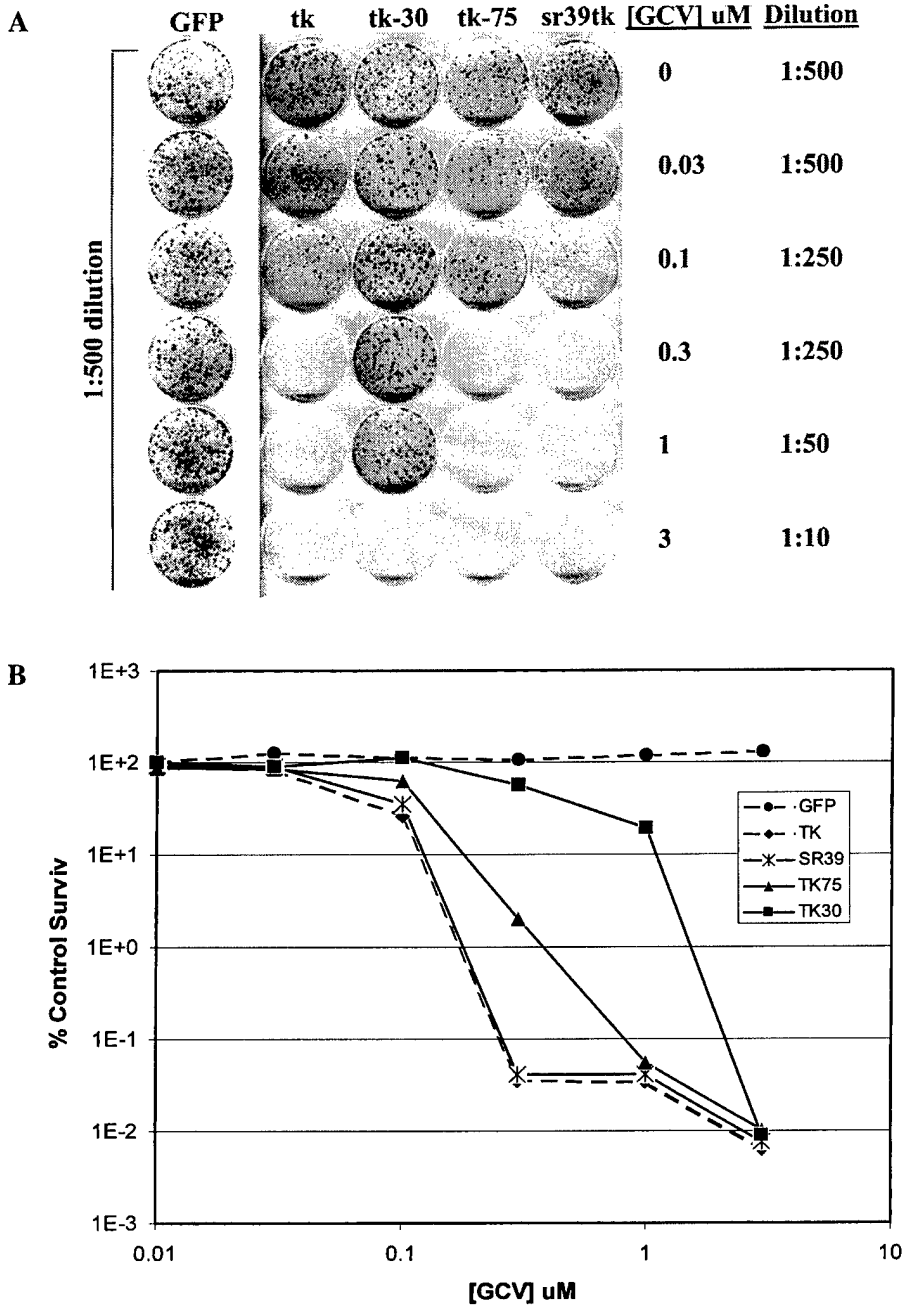

FIG. 2. *In vitro* cytotoxicity assays in infected CL1 cells mediated by GCV dose escalation. (**A** and **B**) Representative results and quantitation of a colony formation assay. Cells were infected as described in Fig. 1. Postinfection (24 hr), cells were aliquoted equivalently into wells containing various concentrations of GCV (0–3 μM, as specified). Four days after drug treatment, cells from each well were trypsinized and replated at low densities to allow formation of distinct colonies (**A**). (**B**) Graphic representation of the viable colonies (30–50 cells) formed approximately 10–14 days postplating. (**C**) MTT assay of infected CL1 cells. Cells were infected at an MOI of 1 with the specified virus. One day postinfection, cells were aliquoted into 24-well plates containing various concentrations of GCV prodrug. Seven days after drug exposure, cells were stained with MTT to score for cytotoxicity, as described in Materials and Methods. Percentages of cell survival were calculated in reference to control. (**D**) Propidium iodide assay to evaluate cell damage. Cell infection and prodrug treatment were as described in (**C**). Five to 7 days after drug exposure, cells were subjected to PI staining and flow cytometry analysis.

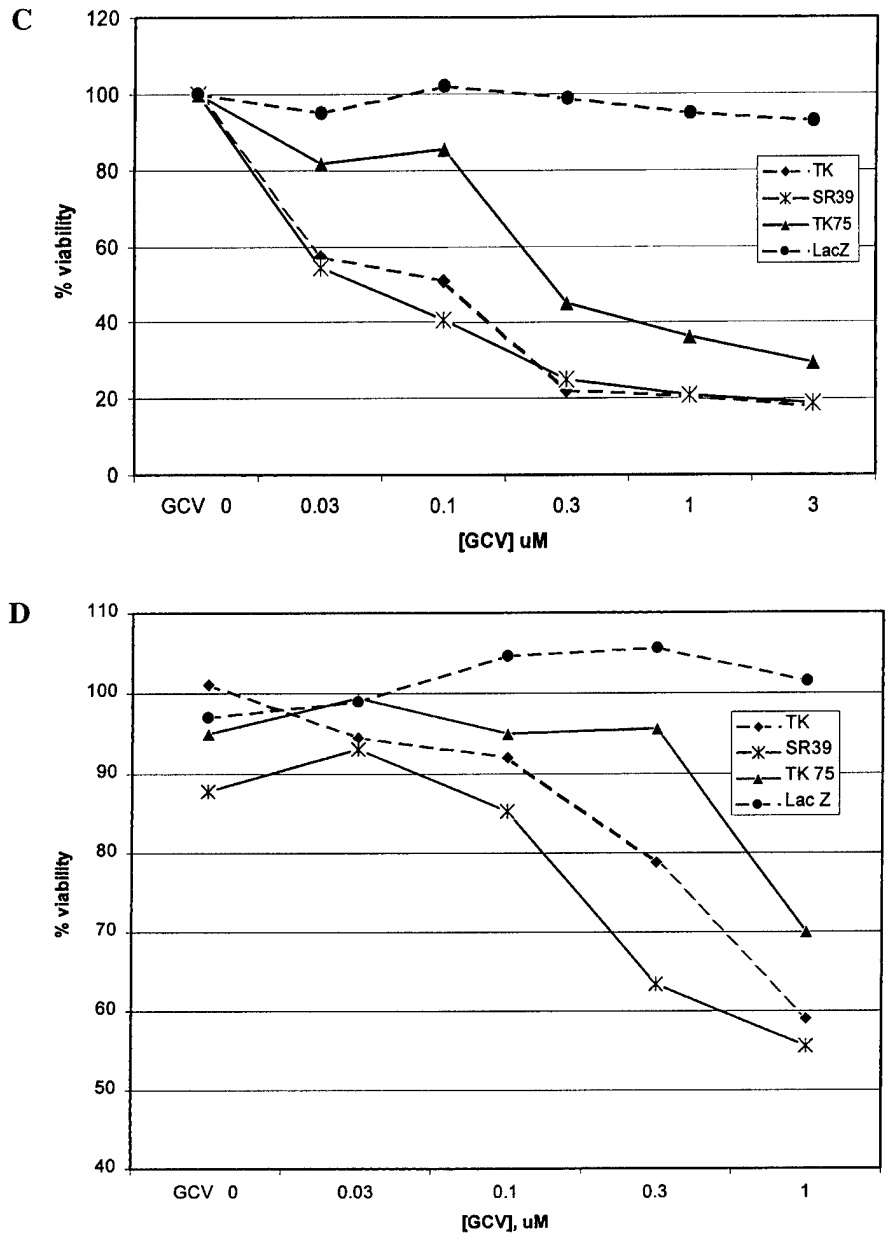

FIG. 2. *Continued.*

strate specificity. These mutants have increased sensitivity to and can preferentially phosphorylate GCV and/or ACV over thymidine, relative to the wild-type TK. Improvement in prodrug-mediated cell killing in transfected cell lines (Kokoris *et al.*, 1999; Black *et al.*, 2001), as well as enhancement of the bystander effect in human tumor cells transduced with a retroviral vector (Qiao *et al.*, 2000), have been demonstrated. Increased killing of human pancreatic tumor cells transfected with tk30 (Howard *et al.*, 2000) and improved radiosensitization of rat glioma cells expressing tk75 (Valerie *et al.*, 2000) have previously been reported. Furthermore, sr39tk has been shown to improve sensitivity, compared with wild-type tk, when used as an imaging reporter gene for noninvasive PET imaging (Gambhir *et al.*, 2000).

To date, no published study has compared the effects and use of these tk mutants comprehensively in prostate cancer gene therapy. Previous *in vitro* studies of ovarian cancer cell lines have suggested differing sensitivities to ACV and GCV (Alvarez and Curiel, 1997). The current study demonstrates that both androgen-dependent and -independent cell lines show greatly increased sensitivity to ACV when infected with an

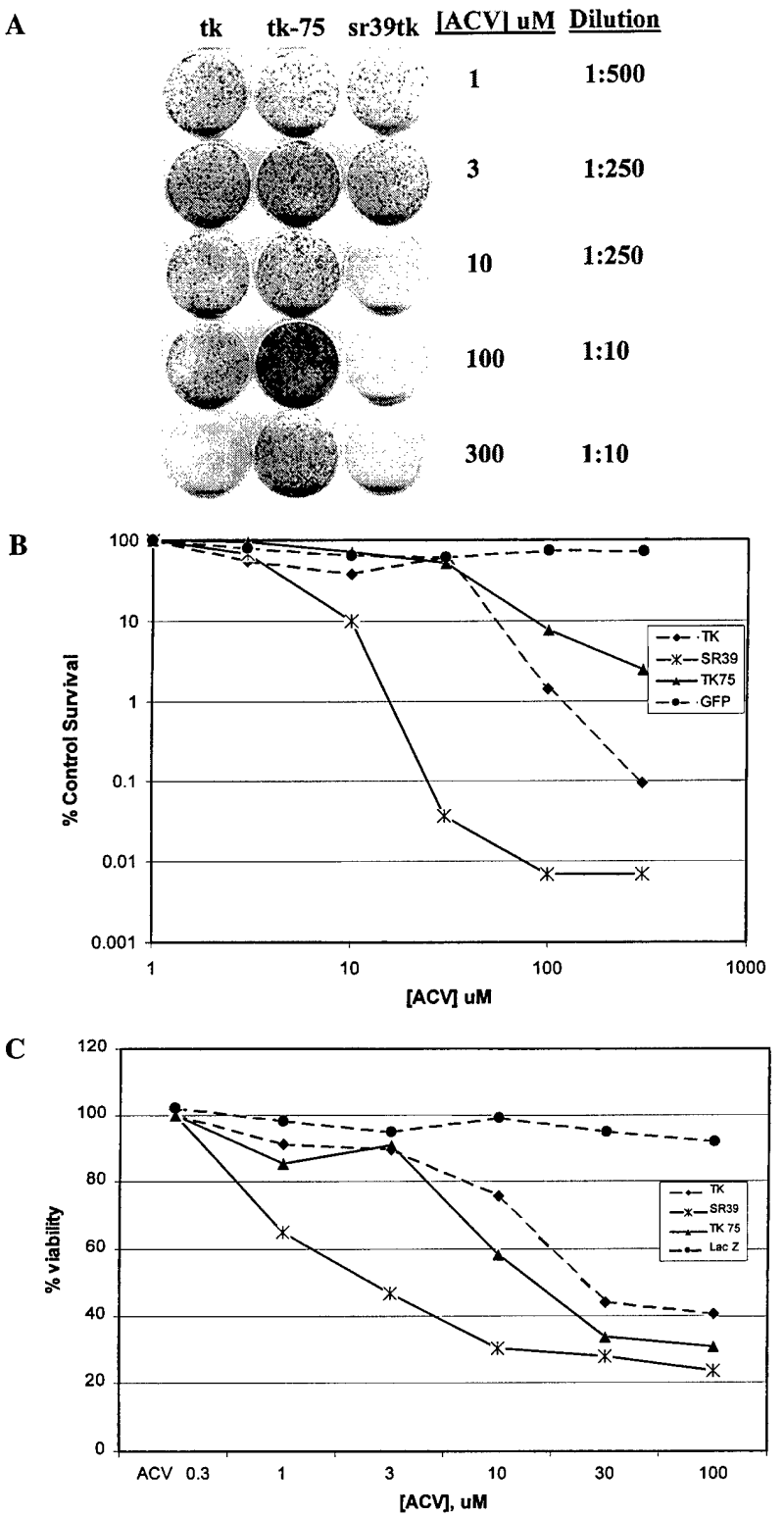

FIG. 3. *In vitro* cytotoxicity in infected CL1 cells mediated by ACV dose escalation. (**A** and **B**) Results of a colony formation assay. Experimental conditions were the same as described in Fig. 2, except that ACV was used instead of GCV at specified dosages. (**C**) MTT assay of infected CL1 cells after ACV treatment. Conditions were as previously described.

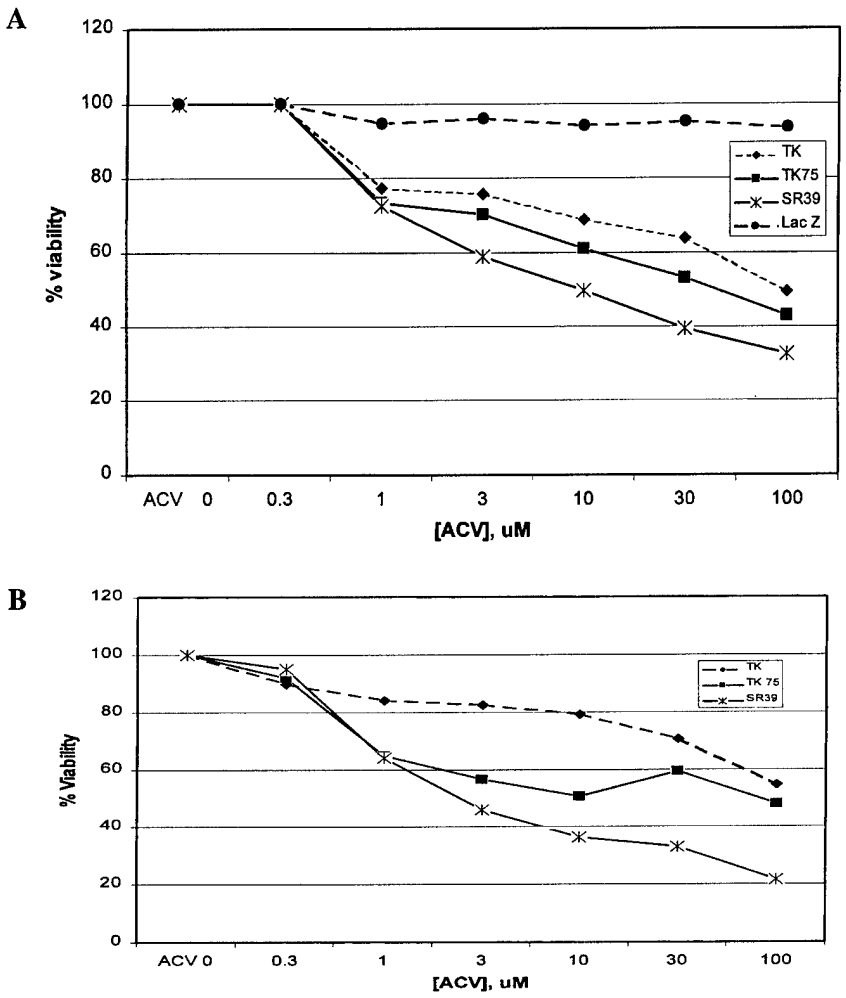

FIG. 4. Cytotoxicity profile of two prostate cancer cell lines treated with tk-expressing Ad and ACV. (**A**) MTT assay of infected DU-145 cells. (**B**) MTT assay of infected LNCaP cells. Conditions were as described in Figs. 2 and 3.

sr39tk-expressing Ad, as compared with wild-type tk, tk75, or tk30. When combined with GCV, wild-type tk and sr39tk display similar levels of *in vitro* killing that are slightly higher than for tk75. A distinct improvement of sr39tk-expressing Ad as compared with wild-type tk-expressing Ad, in conjunction with GCV treatment, is suppression of metastatic spread of the infected prostate cancer cells. This result in animals is unexpected because the cytotoxicity of GCV treatment in tissue culture systems showed no notable difference in sr39 tk-expressing CL1 cells over wild type. In the well-controlled tissue culture studies, prodrug delivery is not rate limiting and TK expression can be accurately assessed. However, in animals, the *in vivo* tissue environment can alter prodrug delivery or its accumulation within tumor cells. Under these limiting conditions, sr39tk could exhibit advantages over wild-type tk. Therefore, sensitive imaging or tracer studies are needed to monitor prodrug accumulation *in situ* in animals to better predict the therapeutic outcome of tk-mediated gene therapy.

Tumor cell eradication was limited in experiments conducted by treating subcutaneous tumors percutaneously injected with Ad carrying tk. Uneven distribution and low gene transduction may be two factors accounting for this limited cytotoxicity. To assess transduction efficiency, we performed percutaneous injections under the same conditions as described in Materials and Methods, with an Ad carrying the gene encoding green fluorescent protein. These experiments showed that distribution of Ad into the CL1 tumors was limited: less than 10% of tumor cells were infected, with a dispersion of only 1 mm beyond the path of the needle track (data not shown). CL1 cells form desmoplastic, densely packed solid tumors. This aggressive CL tumor model (Patel *et al.*, 2000; Tso *et al.*, 2000) is highly tumorigenic, and exhibits rapid growth, local invasion, and metastatic spread in the absence of androgen or other growth supplementation (e.g., Matrigel). In light of this combination of limited transduction efficacy and a rapidly growing tumor model, effective *in vivo* cytoxicity will likely require the ability to augment the bystander

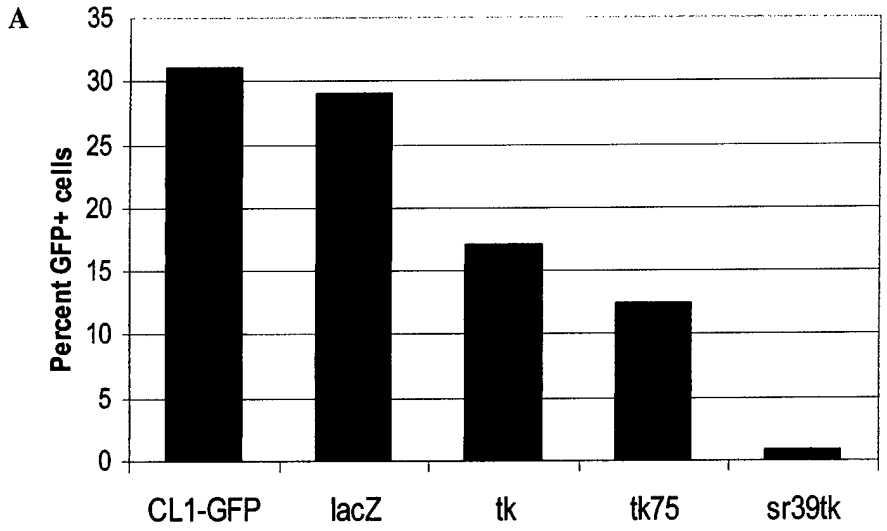

FIG. 5. Detection of metastatic CL1-GFP cells by fluorescence. (**A**) Liver sections were enzymatically digested and subjected to FACS analysis to determine the percentages of GFP-expressing prostate cancer cells (see Materials and Methods for a more detailed description). (**B**) Microscopy of liver sections obtained at sacrifice shows GFP-expressing, metastatic prostate cancer cells. CL1-GFP cells were infected with tk-expressing Ad at an MOI of 1. One day postinfection, 5×10^4 cells were injected orthotopically into the prostate (dorsal lobe) of SCID mice. Mice were treated with systemic GCV administration for 6 days. Three weeks after implantation of infected CL1-GFP cells (tumors were palpable), all animals were killed, and frozen sections of liver were visualized under a fluorescence microscope. Untreated CL1 tumors revealed macroscopic liver metastases. Mice receiving cells treated with wild-type tk- or tk75-expressing Ad revealed diffuse, microscopic metastases. Liver sections of mice receiving cells treated with sr39tk-expressing Ad showed minimal microscopic metastasis.

effect (Mesnil and Yamasaki, 2000) or intercellular spread of activating enzyme (Dilber *et al.*, 1999).

Another issue that is unclear at this time is whether improvement in TK enzyme kinetics can be translated into improved cytotoxicity. Enhanced substrate uptake by SR39 TK enzyme as compared with wild-type TK has been documented with tritiated PCV and ^{18}F-labeled PCV (FPCV), which resulted in improved sensitivity of PET imaging (Gambhir *et al.*, 2000). C6 rat glioma cells stably expressing SR39 were shown to be more sensitive to GCV-mediated tumor growth suppression compared with wild-type TK-expressing tumors (Black *et al.*, 2001). Two factors could contribute to the difference between our results and those reported in the study by Black *et al.* As alluded to previously, our tk gene transduction is mediated by an Ad that does not confer stable tk expression. Thus, delivery and expression could be limiting factors *in vivo*. Another possibility that could explain why apparently improved TK enzyme kinetics fail to correlate with substantially improved cytotoxicity in our system is that the cytotoxic effect is more complicated than just one enzyme–ligand interaction. TK enzyme activity measures the conversion of the nucleoside into the monophosphate form, which is the first form that becomes trapped in the cell, and therefore can be used as a PET reporter probe (Gambhir *et al.*, 1999). Studies have demonstrated that GCV incorporation in the DNA template was important for cytotoxicity (Rubsam *et al.*, 1999; Thust *et al.*, 2000). It is possible that different cell types could have differential abilities to convert the nucleoside monophosphates into the triphosphate forms or the form that causes cytotoxicity. These are issues that need to be clarified for individual cell systems, in order to achieve optimal TK-mediated cytotoxicity. Further improvement in TK enzyme activity or novel prodrug substrates with enhanced toxicity should augment the efficacy of tk suicide gene-based cancer treatment strategies.

One approach to investigate treatment failure is to noninvasively assay transgene expression, such that correlation of the level of transgene expression and the observed cytotoxic effect can be established. As a first step to achieving this end, we stably transfected the CL1 tumor model with the sr39tk gene. These data suggest that micro-PET imaging can be used as a means to selectively image prostate cancer cells carrying the sr39tk gene, similar to other tumor models (Gambhir *et al.*, 2000). The CL1-sr39tk tumor model can be repetitively imaged, and may prove to be useful for studies of the biology of metastasis, as well as for noninvasive evaluation of therapeutic interventions. In conclusion, *in vitro* and *in vivo* suicide gene therapy studies of an androgen-independent model of metastatic prostate cancer, using a panel of variant HSV1 tk genes in combination with ACV and GCV prodrugs, suggest the advantage of using sr39tk versus wild-type tk. The use of sr39tk for future clinical prostate cancer gene therapy trials might enhance cytotoxic effects and suppress metastatic spread.

ACKNOWLEDGMENTS

This study is supported by the California Cancer Research Program (L.W., 99-00579V-10191) and the U.S. Department

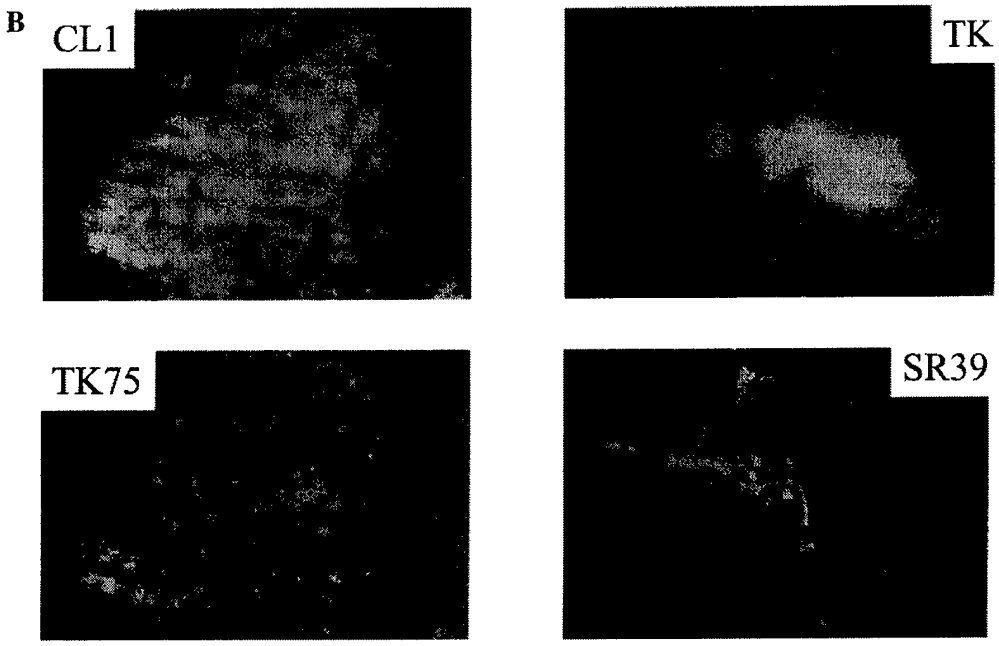

4C
FPO

FIG. 5B.

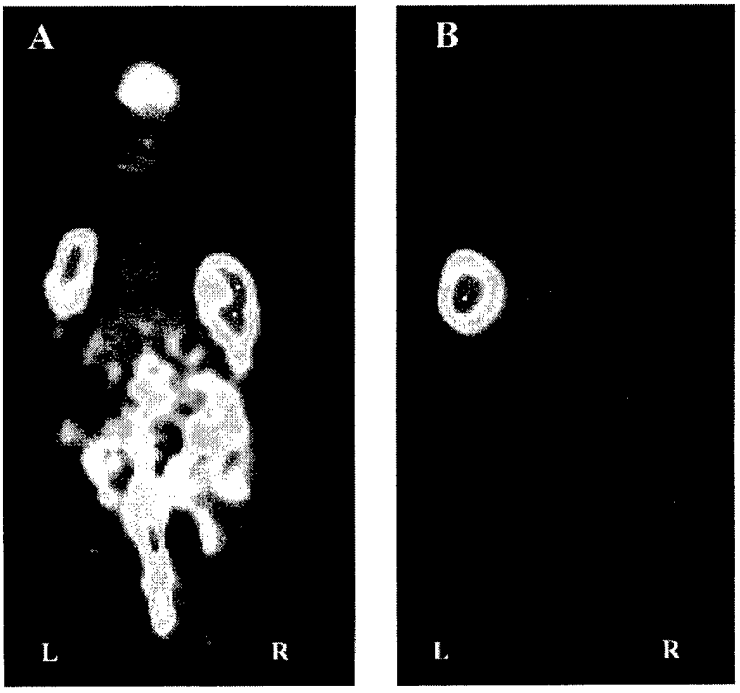

4C
FPO

FIG. 6. Micro-PET images of mice xenografted with CL1 cells or CL1 stably expressing the sr39tk gene. (**A**) Image visualized with FDG as PET reporter substrate. Both CL1 and CL1-sr39tk xenografts were visualized, indicating comparable glucose metabolism. (**B**) PET image of the same mouse, visualized with FHBG as substrate. Only the CL1-sr39tk tumor phosphorylates and retains FHBG in the cells. A robust signal was produced by the sr39tk-expressing tumor, whereas only background signal was seen from the site of the CL1 tumor.

of the Army (A.B. and L.W., DAMD17-PC000046). The Jonsson Comprehensive Cancer Center and the Carolan Foundation at UCLA provided seed funding for this project. The imaging work is supported in part by NIH grants P50 CA86306 (S.S.G.) and SAIRP R24 CA92865 (S.S.G.), and by Department of Energy contract DE-FC03-87ER60615 (S.S.G.). We deeply appreciated the support of the Human Gene Medicine program at UCLA (A.P. and L.W.), and are indebted to Dr. Harvey Herschman for advice, and for providing AdCMV-HSV1-sr39tk. We appreciate the technical assistance from Erika Billick and Dr. Sun Paik, Dr. Ke-Hung Tsui in animal studies, and Wendy Aft in manuscript preparation.

REFERENCES

ALVAREZ, R.D., and CURIEL, D.T. (1997). A phase I study of recombinant adenovirus vector-mediated intraperitoneal delivery of herpes simplex virus thymidine kinase (HSV-TK) gene and intravenous ganciclovir for previously treated ovarian and extraovarian cancer patients. Hum. Gene Ther. **8,** 597–613.

BELLDEGRUN, A., TSO, C.L., ZISMAN, A., NAITOH, J., SAID, J., PANTUCK, A.J., HINKEL, A., DEKERNION, J., and FIGLIN, R. (2001). Interleukin 2 gene therapy for prostate cancer: Phase I clinical trial and basic biology. Hum. Gene Ther. **12,** 883–892.

BLACK, M.E., NEWCOMB, T.G., WILSON, H.M., and LOEB, L.A. (1996). Creation of drug-specific herpes simplex virus type 1 thymidine kinase mutants for gene therapy. Proc. Natl. Acad. Sci. U.S.A. **93,** 3525–3529.

BLACK, M.E., KOKORIS, M.S., and SABO, P. (2001). Herpes simplex virus-1 thymidine kinase mutants created by semi-random sequence mutagenesis improve prodrug-mediated tumor cell killing. Cancer Res. **61,** 3022–3026.

BLACKBURN, R.V., GALOFORO, S.S., CORRY, P.M., and LEE, Y.J. (1998). Adenoviral-mediated transfer of a heat-inducible double suicide gene into prostate carcinoma cells. Cancer Res. **58,** 1358–1362.

DILBER, M.S., PHELAN, A., AINTS, A., MOHAMED, A.J., ELLIOTT, G., SMITH, C.I., and O'HARE, P. (1999). Intercellular delivery of thymidine kinase prodrug activating enzyme by the herpes simplex virus protein, VP22. Gene Ther. **6,** 12–21.

DORAI, T., OLSSON, C.A., KATZ A.E., and BUTTYAN, R. (1997). Development of a hammerhead ribozyme against bcl-2. I. Preliminary evaluation of a potential gene therapeutic agent for hormone-refractory human prostate cancer. Prostate **32,** 246–258.

EASTHAM, J.A., HALL, S.J., SEHGAL, I., WANG, J., TIMME, T.L., YANG, G., CONNELL-CROWLEY, L., ELLEDGE, S.J., ZHANG, W.W., and HARPER, J.W. (1995). In vivo gene therapy with p53 or p21 adenovirus for prostate cancer. Cancer Res. **55,** 5151–5155.

EASTHAM, J.A., CHEN, S.H., SEHGAL, I., YANG, G., TIMME, T.L., HALL, S.J., WOO, S.L., and THOMPSON, T.C. (1996). Prostate cancer gene therapy: Herpes simplex virus thymidine kinase gene transduction followed by ganciclovir in mouse and human prostate cancer models. Hum. Gene Ther. **7,** 515–523.

GAMBHIR, S.S., BARRIO, J.R., PHELPS M.E., IYER, M., NAMAVARI, M., SATYAMURTHY, N., WU, L., GREEN, L.A., BAUER, E., MACLAREN, D.C., NGUYEN, K., BERK, A.J., CHERRY, S.R., and HERSCHMAN, H.R. (1999). Imaging adenoviral-directed reporter gene expression in living animals with positron emission tomography. Proc. Natl. Acad. Sci. U.S.A. **96,** 2333–2338.

GAMBHIR, S.S., BAUER, E., BLACK, M.E., LIANG, Q., KOKORIS, M.S., BARRIO, J.R., IYER, M., NAMAVARI, M., PHELPS, M.E., and HERSCHMAN, H.R. (2000). A mutant herpes simplex virus type 1 thymidine kinase reporter gene shows improved sensitivity for imaging reporter gene expression with positron emission tomography. Proc. Natl. Acad. Sci. U.S.A. **97,** 2785–2790.

HALL, S.J., MUTCHNIK, S.E., CHEN, S.H., WOO, S.L., and THOMPSON, T.C. (1997). Adenovirus-mediated herpes simplex virus thymidine kinase gene and ganciclovir therapy leads to systemic activity against spontaneous and induced metastasis in an orthotopic mouse model of prostate cancer. Int. J. Cancer **70,** 183–187.

HASSAN, W., SANFORD, M.A., WOO, S.L., CHEN, S.H., and HALL, S.J. (2000). Prospects for herpes-simplex-virus thymidine-kinase and cytokine gene transduction as immunomodulatory gene therapy for prostate cancer. World J. Urol. **18,** 130–135.

HERMAN, J.R., ADLER, H.L., AGUILAR-CORDOVA, E., ROJAS-MARTINEZ, A., WOO, S., TIMME, T.L., WHEELER, T.M., THOMPSON, T.C., and SCARDINO, P.T. (1999). In situ gene therapy for adenocarcinoma of the prostate: A phase I clinical trial. Hum. Gene Ther. **10,** 1239–1249.

HOWARD, B.D., BOENICKE, L., SCHNIEWIND, B., HENNE-BRUNS, D., and KALTHOFF, H. (2000). Transduction of human pancreatic tumor cells with vesicular stomatitis virus G-pseudotyped retroviral vectors containing a herpes simplex virus thymidine kinase mutant gene enhances bystander effects and sensitivity to ganciclovir. Cancer Gene Ther. **7,** 927–938.

KOKORIS, M.S., SABO, P., ADMAN, E.T., and BLACK, M.E. (1999). Enhancement of tumor ablation by a selected HSV-1 thymidine kinase mutant. Gene Ther. **6,** 1415–1426.

LANDIS, S.H., MURRAY, T., BOLDEN, S., and WINGO, P.A. (1999). Cancer statistics, 1999. CA Cancer J. Clin. **49,** 8–31.

MACLAREN, D.C., GAMBHIR, S.S., SATYAMURTHY, N., BARRIO, J.R., SHARFSTEIN, S., TOYOKUNI, T., WU, L., BERK, A.J., CHERRY, S.R., PHELPS, M.E., and HERSCHMAN, HR. (1999). Repetitive, non-invasive imaging of the dopamine D2 receptor as a reporter gene in living animals. Gene Ther. **6,** 785–791.

MESNIL, M., and YAMASAKI, H. (2000). Bystander effect in herpes simplex virus-thymidine kinase/ganciclovir cancer gene therapy: Role of gap-junctional intercellular communication. Cancer Res. **60,** 3989–3999.

PATEL, B.J., PANTUCK, A.J., ZISMAN, A., TSUI, K.H., PAIK, S.H., CALILIW, R., SHERIFF, S., WU, L., DEKERNION, J.B., TSO, C.L., and BELLDEGRUN, A.S. (2000). CL1-GFP: An androgen independent metastatic tumor model for prostate cancer. J. Urol. **164,** 1420–1425.

QI, J., LEAHY, R.M., CHERRY, S.R., CHATZIIOANNOU, A., and FARQUHAR, T.H. (1998). High-resolution 3D Bayesian image reconstruction using the microPET small-animal scanner. Phys. Med. Biol. **43,** 1001–1013.

QIAO, J., BLACK, M.E., and CARUSO, M. (2000). Enhanced ganciclovir killing and bystander effect of human tumor cells transduced with a retroviral vector carrying a herpes simplex virus thymidine kinase gene mutant. Hum. Gene Ther. **11,** 1569–1576.

RUBSAM, L.Z., BOUCHER, P.D., MURPHY, P.J., KUKURUGA, M., and SHEWACH, D.S. (1999). Cytotoxicity and accumulation of ganciclovir triphosphate in bystander cells cocultured with herpes simplex virus type 1 thymidine kinase-expressing human glioblastoma cells. Cancer Res. **59,** 669–675.

SHALEV, M., MILES, B.J, THOMPSON, T.C., AYALA, G., BUTLER, E.B., AGUILAR-CORDOVA, E., and KADMON, D. (2000). Suicide gene therapy for prostate cancer using a replication-deficient adenovirus containing the herpesvirus thymidine kinase gene. World J. Urol. **18,** 125–129.

SIMONS, J.W., MIKHAK, B., CHANG, J.F., DEMARZO, A.M., CARDUCCI, M.A., LIM, M., WEBER, C.E., BACCALA, A.A., GOEMANN, M.A., CLIFT, S.M., ANDO, D.G., LEVITSKY, H.I., COHEN, L.K., SANDA, M.G., MULLIGAN, R.C., PARTIN, A.W., CARTER, H.B., PIANTADOSI, S., MARSHALL, F.F., and NELSON, W.G. (1999). Induction of immunity to prostate cancer antigens: Results of a clinical trial of vaccination with irradiated autol-

ogous prostate tumor cells engineered to secrete granulocyte-macrophage colony-stimulating factor using ex vivo gene transfer. Cancer Res. **59,** 5160–5168.

SOKOLOFF, M.H., TSO, C.L., KABOO, R., TANEJA, S., PANG, S., DEKERNION, J.B., and BELLDEGRUN, A.S. (1996). In vitro modulation of tumor progression-associated properties of hormone refractory prostate carcinoma cell lines by cytokines. Cancer **77,** 1862–1872.

TAN, B.T., WU, L., and BERK, A.J. (1999). An adenovirus–Epstein-Barr virus hybrid vector that stably transforms cultured cells with high efficiency. J. Virol. **73,** 7582–7589.

THUST, R., TOMICIC, M., KLOCKING, R., VOUTILAINEN, N., WUTZLER, P., and KAINA, B. (2000). Comparison of the genotoxic and apoptosis-inducing properties of ganciclovir and penciclovir in Chinese hamster ovary cells transfected with the thymidine kinase gene of herpes simplex virus-1: Implications for gene therapeutic approaches. Cancer Gene Ther. **7,** 107–117.

TSO, C.L., MCBRIDE, W.H., SUN, J., PATEL, B., TSUI, K.H., PAIK, S.H., GITLITZ, B., CALILIW, R., VAN OPHOVEN, A., WU, L., DEKERNION, J., and BELLDEGRUN, A. (2000). Androgen deprivation induces selective outgrowth of aggressive hormone-refractory prostate cancer clones expressing distinct cellular and molecular properties not present in parental androgen-dependent cancer cells. Cancer J. **6,** 220–233.

VALERI, K., BRUST, D., FARNSWORTH, J., AMIR, C., TAHER, M.M., HERSHEY, C., and FEDEN, J. (2000). Improved radiosensitization of rat glioma cells with adenovirus-expressed mutant herpes simplex virus-thymidine kinase in combination with acyclovir. Cancer Gene Ther. **7,** 879–884.

VIEWEG, J., ROSENTHAL, F.M., BANNERJI, R., HESTON, W.D., FAIR, W.R., GANSBACHER, B., and GILBOA, E. (1994). Immunotherapy of prostate cancer in the Dunning rat model: Use of cytokine gene modified tumor vaccines. Cancer Res. **54,** 1760–1765.

WALLACE, H., CLARKE, A.R., HARRISON, D.J., HOOPER, M.L., and BISHOP, J.O. (1996). Ganciclovir-induced ablation non-proliferating thyrocytes expressing herpesvirus thymidine kinase occurs by p53-independent apoptosis. Oncogene **13,** 55–61.

Address reprint requests to:
Dr. Lily Wu
Department of Urology
MRL 2210, Box 951738
University of California Los Angeles School of Medicine
Los Angeles, CA 90095-1738

E-mail: lwu@mednet.ucla.edu

Received for publication November 2, 2001; accepted after revision March 5, 2002.

Published online: XXXXX.

AU 1
No Morelli *et al.* (1997) in reference list?

AU 2
Preceding sentence OK as edited? Or please amend to clarify meaning.